

# Day 3. Machine Learning of Spectroscopic Data Sets

Sergei V. Kalinin

# Linear Unmixing Methods

## 1. Why linear unmixing?

- Spectral images
- Image analysis

## 2. Multiple linear regression

## 3. Principal component analysis (PCA)

- Definition and implementation
- PCA for scanning tunneling microscopy
- Physical meaning of PCA: band excitation SPM
- PCA on imaging data

## 4. Independent component analysis (ICA)

## 5. N-FINDR and Bayesian linear unmixing

- Mapping phase transitions
- Image segmentation

Physical constraints in linear models: **If solution exists and its unique, doesn't matter how you find it**

# Spectroscopic Imaging

## Scanning probe microscopy:

- Force-distance curve measurements
- Current-voltage measurements
- Piezoresponse force/electrochemical strain spectroscopy

## Electron microscopy:

- Electron Energy Loss Spectroscopy

## Optical microscopy:

- Hyperspectral imaging
- Time resolved measurements

## Mass-spectrometry:

- Secondary ion MS imaging

In many cases, measured signal can be represented or approximated as a linear combination of signals. However, their functional forms are generally unknown

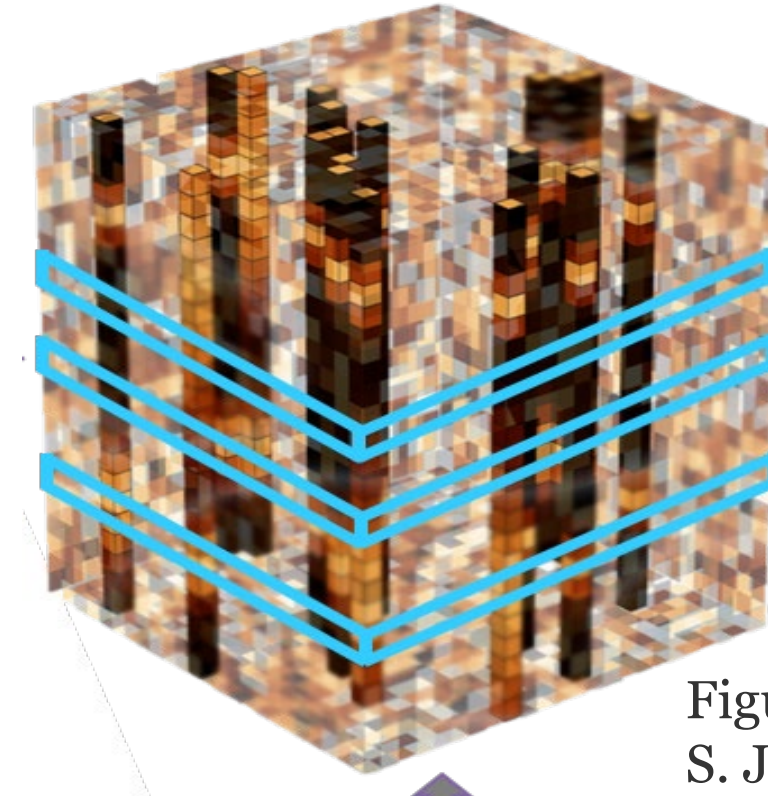
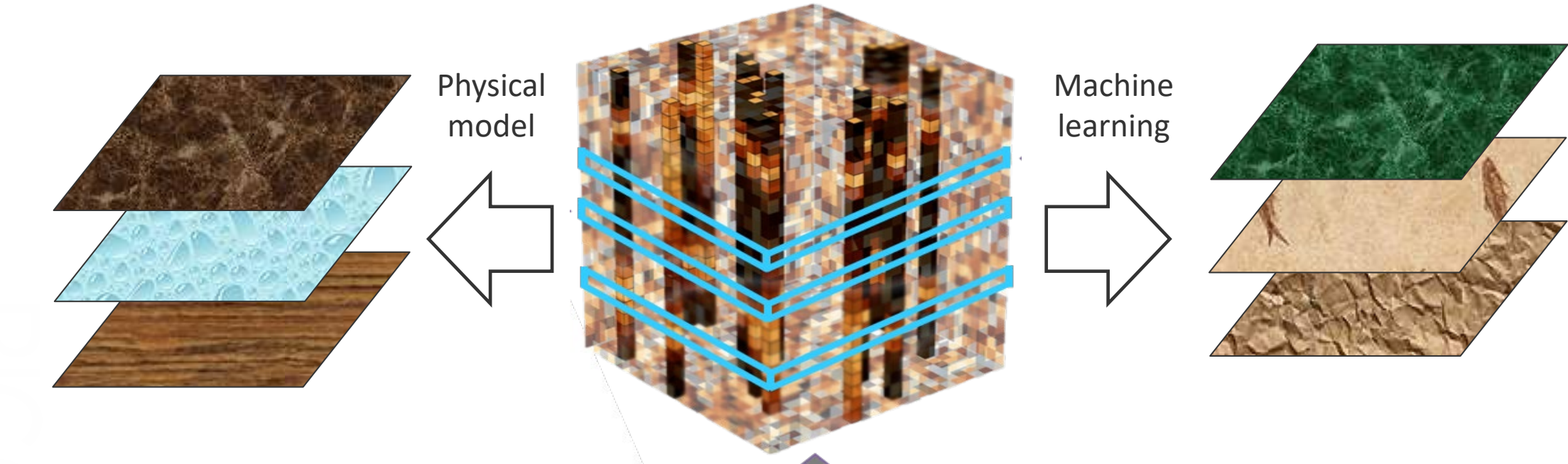


Figure by  
S. Jesse

Very important: convolution with resolution function is also mixing

# Physics vs. ML based analysis



- If we have physical model, we can extract relevant parameters from data
- Imperfect model: epistemic uncertainty
- Noisy data: aleatoric uncertainty
- Analysis results do not depend on sampling of data in  $x,y$
- If we don't have physical model, we can learn intrinsic structure of data
- **Unsupervised learning:** based on data only
  - But not really (definition of distance)
  - Analysis can depend on sampling of data
- **Supervised learning:** based on prior examples
  - Out of distribution shifts

**Physics-informed ML:** Combines strengths (and limitations) of both approaches

# General linear unmixing

$$S(\mathbf{x}, \mathbf{R}) = \sum_i a_i(\mathbf{x}) w_i(\mathbf{R}) + N$$

**We start with:**

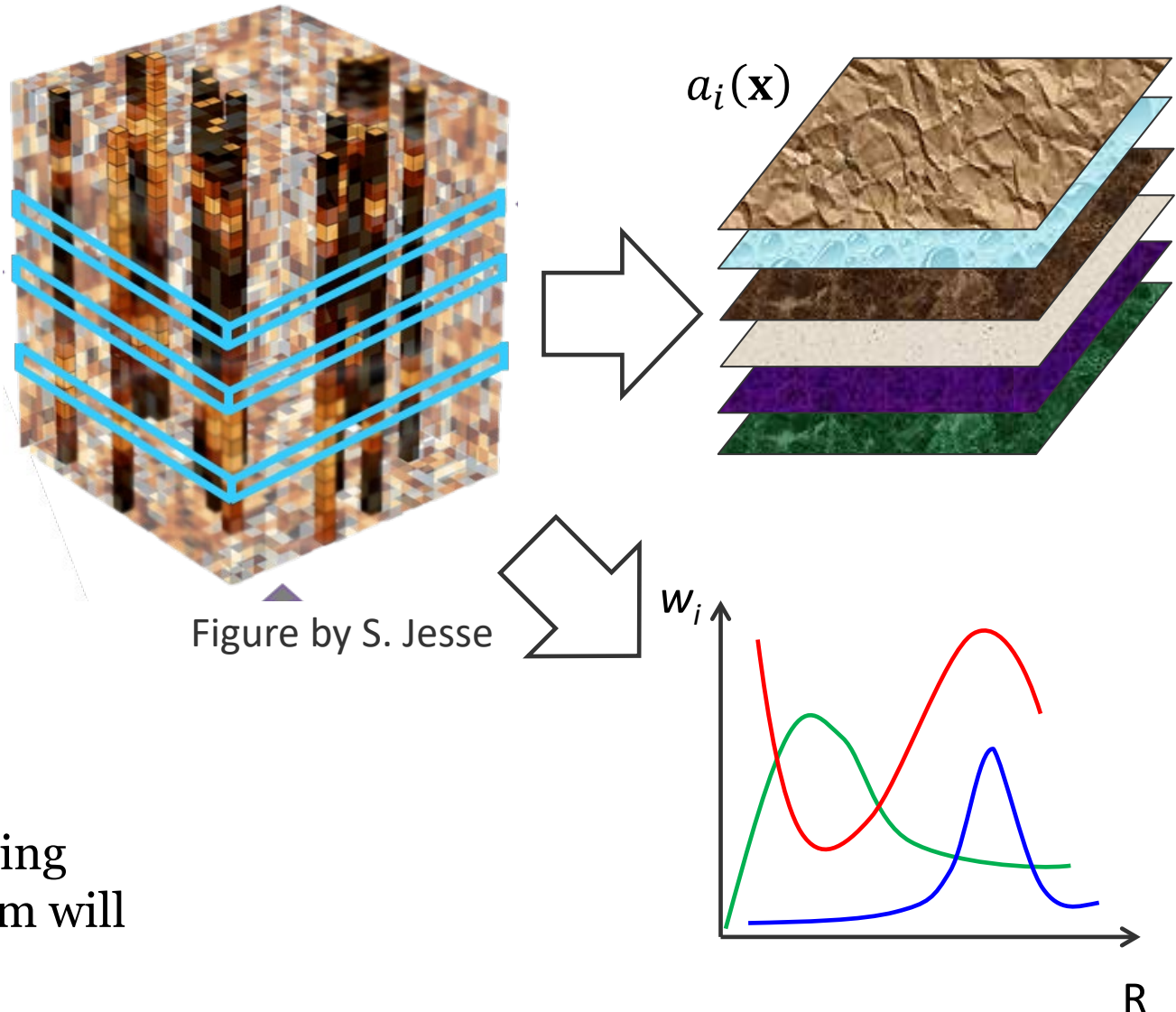
- $\mathbf{x}$  is the spatial variable,  $\mathbf{x} = (x, y)$
- $\mathbf{R}$  is the (vector) parameter variable

Overall, for  $M \times M$  image and  $P$  point in spectra, we have  $M^2 P$  data points

**We aim to get:**

- $a_i(\mathbf{x})$  are loading maps
- $w_i(\mathbf{R})$  are endmembers/eigenvectors
- $N$  is noise

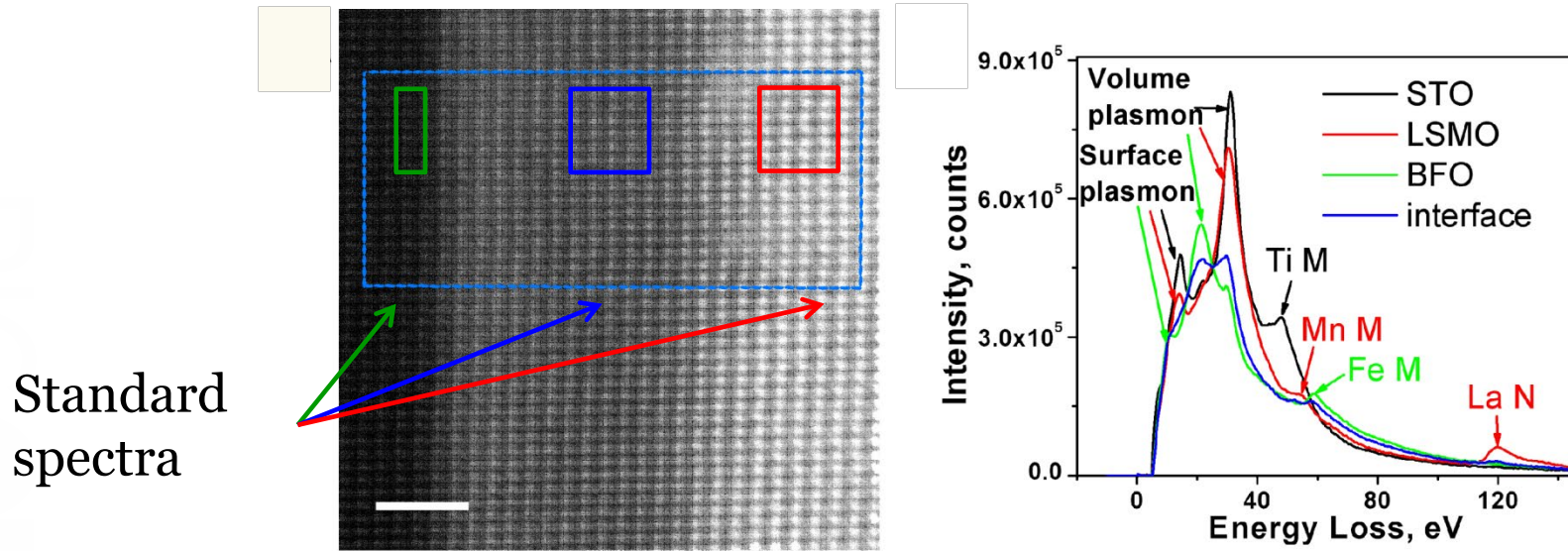
Overall, we can have (maximum)  $P$  loading maps of  $M^2$  size. However, not all of them will have useful information



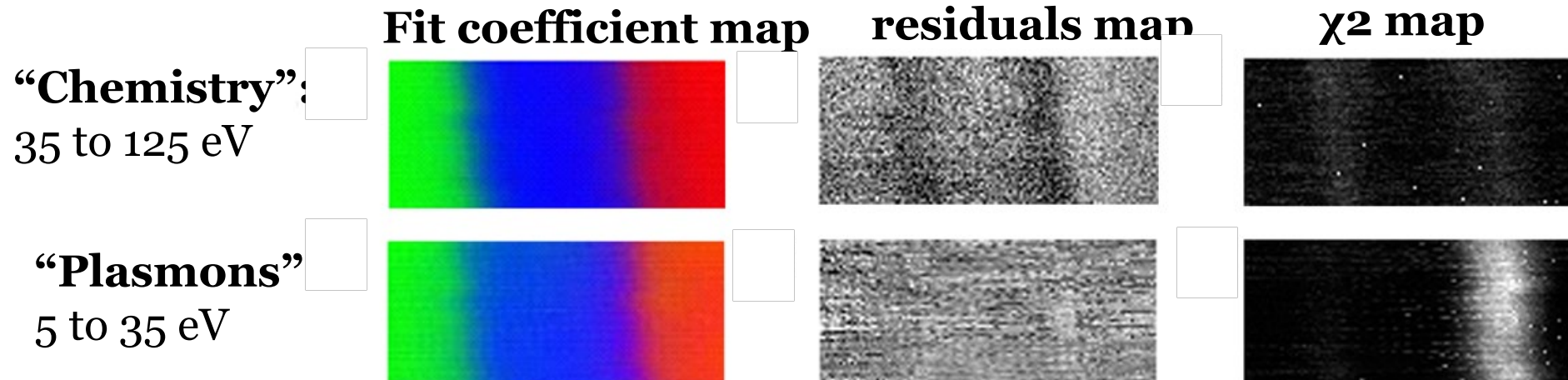
# Multiple Linear Regression

Linear mixing  $S(\mathbf{x}, \mathbf{R}) = \sum_i a_i(\mathbf{x}) w_i(\mathbf{R}) + N$  but  $w_i(\mathbf{R})$  are known

## STEM of STO/LSMO/BFO interface    Low-loss EELS spectra of three components



A.Y. BORISEVICH ET AL,  
*Suppression of Octahedral  
Tilts and Associated  
Changes in Electronic  
Properties at Epitaxial  
Oxide Heterostructure  
Interfaces*, Phys. Rev. Lett.  
105, 087204 (2010).



# Principal Component Analysis

$$S(\mathbf{x}, \mathbf{R}) = \sum_i a_i(\mathbf{x}) w_i(\mathbf{R})$$

- In PCA, the eigenvectors  $w_i(\mathbf{R})$  are orthonormal and are arranged such that corresponding eigenvalues are placed in descending order by variance
- Can be used to separate “real data” from “noise” – but needs cut-off/selection criteria
- PCA eigenvectors generally do not have defined physical meaning
- PCA is a starting point for many other unmixing methods

## EELS elemental mapping with unconventional methods I. Theoretical basis: image analysis with multivariate statistics and entropy concepts

Pierre Trebbia \*

Laboratoire de Physique des Solides, Bâtiment 510, F-91405 Orsay Cedex, France

and

Noël Bonnet

Unité INSERM 314 et Université de Reims, 21 rue Clément Ader, F-51100 Reims, France

Received 7 June 1990

Electron energy loss filtered images recorded within a transmission analytical electron microscope are now widely used for the mapping of the elemental distribution of a given atomic species in a specimen prepared as a thin film. Such an image processing may produce both valuable results and artifacts if a careful inspection of all the hypotheses needed by the calculation is not carried out. This paper presents some general statistical methods for a contrast information analysis of a noisy image data set. After a brief introduction of different concepts such as contrast, variance, information and entropy, two unconventional approaches for image analysis are explained: the relative entropy computed with respect to a pure random and signal-free image and the factorial analysis of correspondence (a branch of multivariate statistics). In the companion article (part II), these concepts are applied to real experiments and the results compared with those obtained with a conventional method. Although electron energy loss spectroscopy is the only technique considered here, these methods for image analysis can be applied to a wide variety of noisy data sets (spectra, images, ...) recorded from various sources (electrons, photons, ...).

Why historical papers matter:

- 165 1. Often contain elementary introductions  
2. Deep insights into principles  
3. Surprisingly prescient predictions  
4. Comparison with the present: see the big picture

“Those who cannot remember the past are condemned to repeat it.”

George Santayana,  
The Life of Reason, 1905



Available online at [www.sciencedirect.com](http://www.sciencedirect.com)



Ultramicroscopy 106 (2006) 1024–1032

---

ultramicroscopy

---

[www.elsevier.com/locate/ultramic](http://www.elsevier.com/locate/ultramic)

## Mapping chemical and bonding information using multivariate analysis of electron energy-loss spectrum images

M. Bosman<sup>a,\*</sup>, M. Watanabe<sup>b</sup>, D.T.L. Alexander<sup>c</sup>, V.J. Keast<sup>a</sup>

<sup>a</sup>Australian Key Centre for Microscopy and Microanalysis, University of Sydney, Sydney, NSW 2006, Australia

<sup>b</sup>Department of Materials Science and Engineering, Lehigh University, Bethlehem, PA 18015, USA

<sup>c</sup>Department of Materials Science and Metallurgy, University of Cambridge, Pembroke St. CB2 3QZ, UK

Received 23 June 2005; received in revised form 26 October 2005; accepted 18 April 2006

---

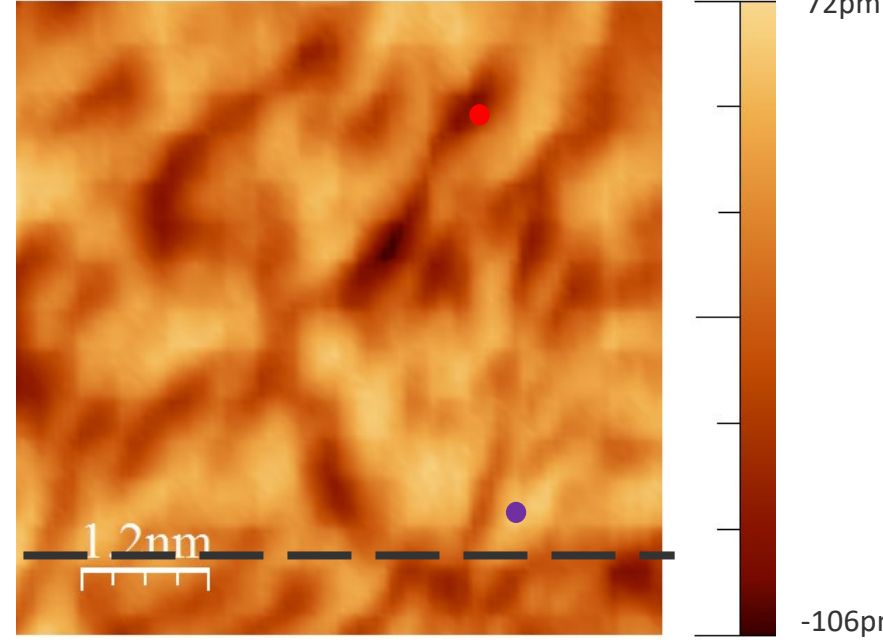
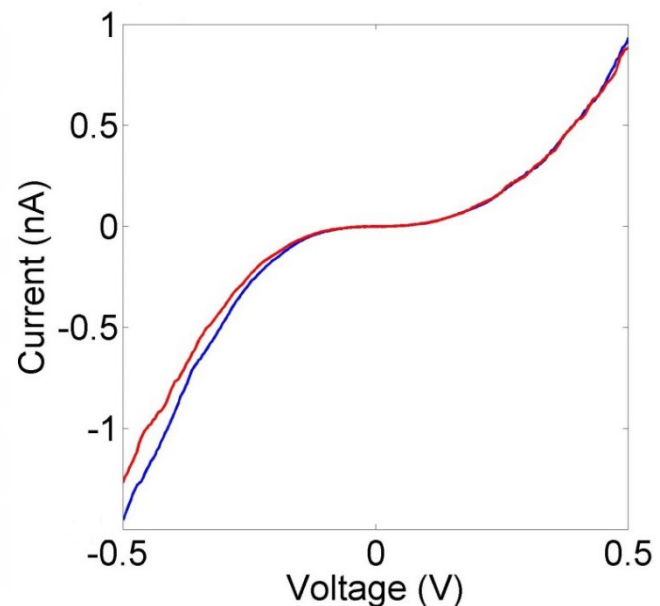
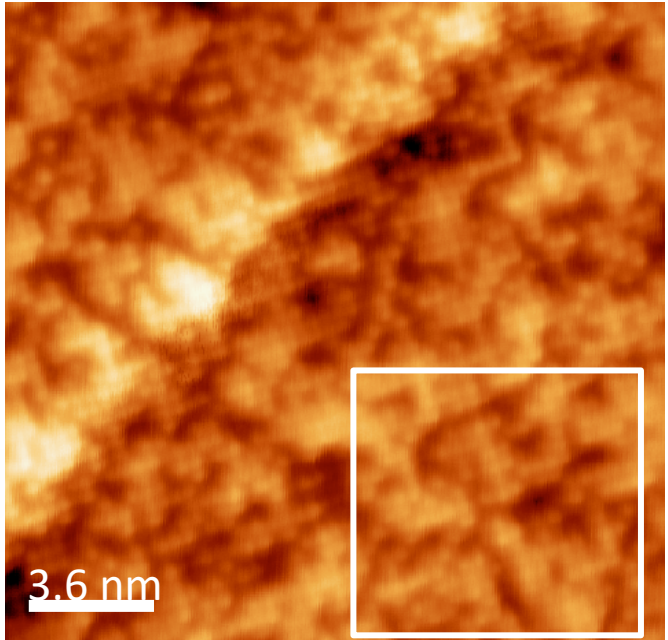
### Abstract

Electron energy-loss spectroscopy (EELS) in the transmission electron microscope (TEM) is used to obtain high-resolution information on the composition and the type of chemical bonding of materials. Spectrum imaging, where a full EEL spectrum is acquired and stored at each pixel in the image, gives an exact correlation of spatial and spectral features. However, determining and extracting the important spectral components from the large amount of information contained in a spectrum image (SI) can be difficult. This paper demonstrates that principal component analysis of EEL SIs can be used to extract chemically relevant components. With weighted or two-way scaled principal component analysis, both compositional and bonding information can be extracted. Mapping of the chemical variations in a partially reduced titanium dioxide sample and the orientation-dependent bonding in boron nitride and carbon nanotubes are given as examples.

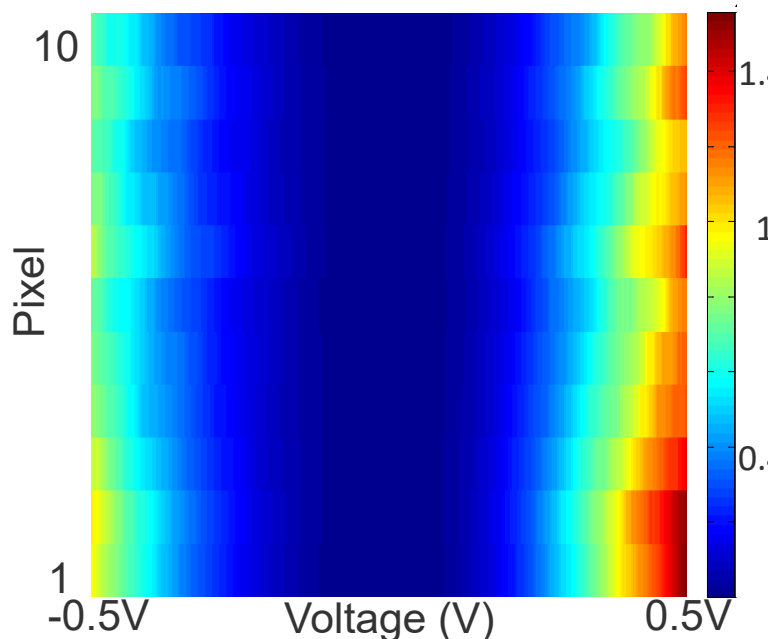
© 2006 Elsevier B.V. All rights reserved.

Why did the PCA on EELS started to grow in 2005 – 2010?

# Grain boundary by STM



Topographical STM of FeSeTe,  $T = 82\text{K}$   $15 \times 15\text{nm}^2$ , 50mV, 100pA, white rectangle represents area where CITS was performed; (b) CITS  $80 \times 80$  pixel graphical average of the spectrographic data.



M. ZIATDINOV, A. MAKSOV, L. LI, A. SEFAT, P. MAKSYMOVYCH, and S.V. KALININ, *Deep data mining in a real space: Separation of intertwined electronic responses in a lightly-doped BaFe<sub>2</sub>As<sub>2</sub>*, Nanotechnology **27**, 475706 (2016).

# Eigenvectors and loadings

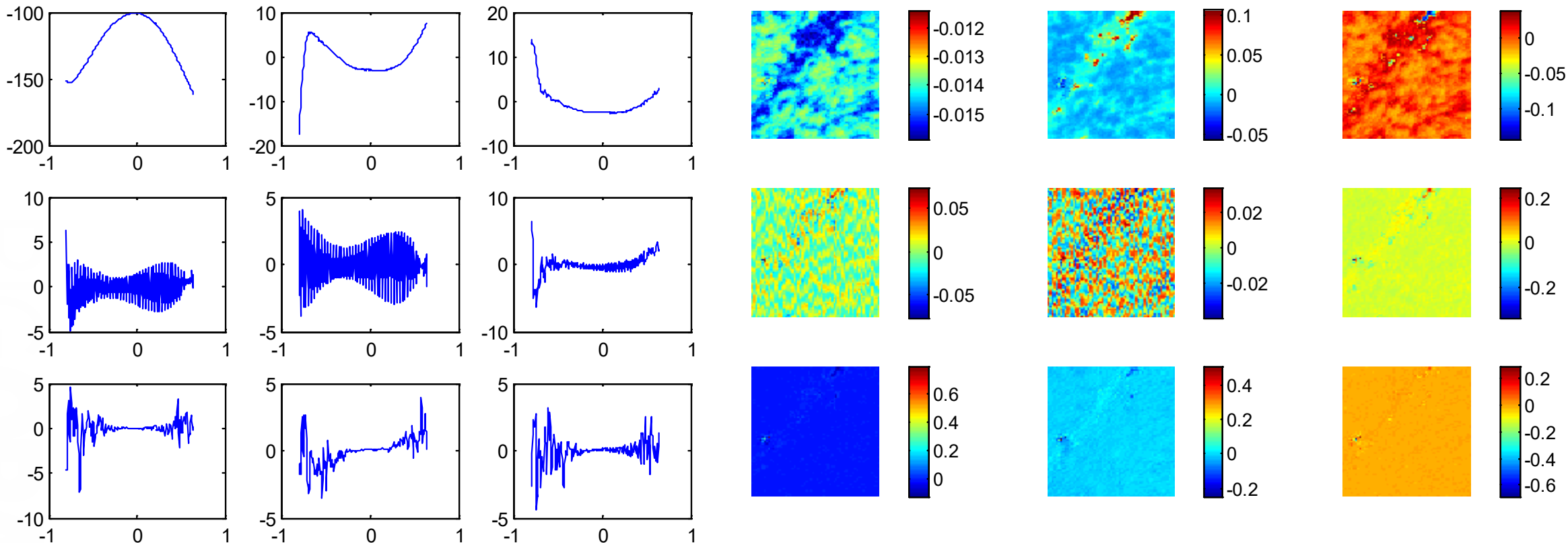


Figure by A. Belianinov

# Scree plot and correlations

- Semi log plot indicating the “weight” of each component as a function of all components
- Only the first few components contain useful info, while others are dominated by noise

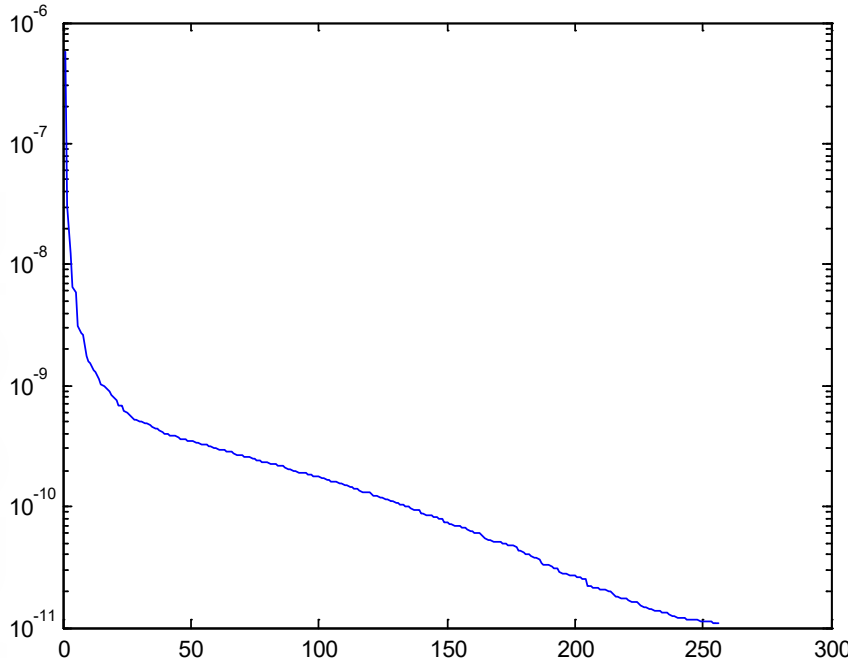
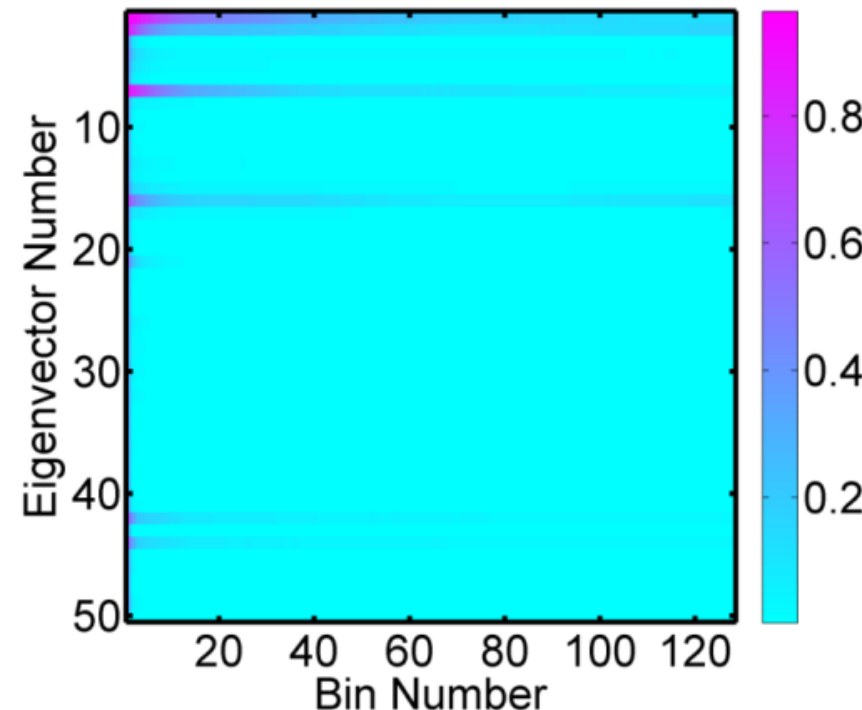


Figure by A. Belianinov

- We can also analyze correlations in images

**For AFM data**

PCA Eigenvectors



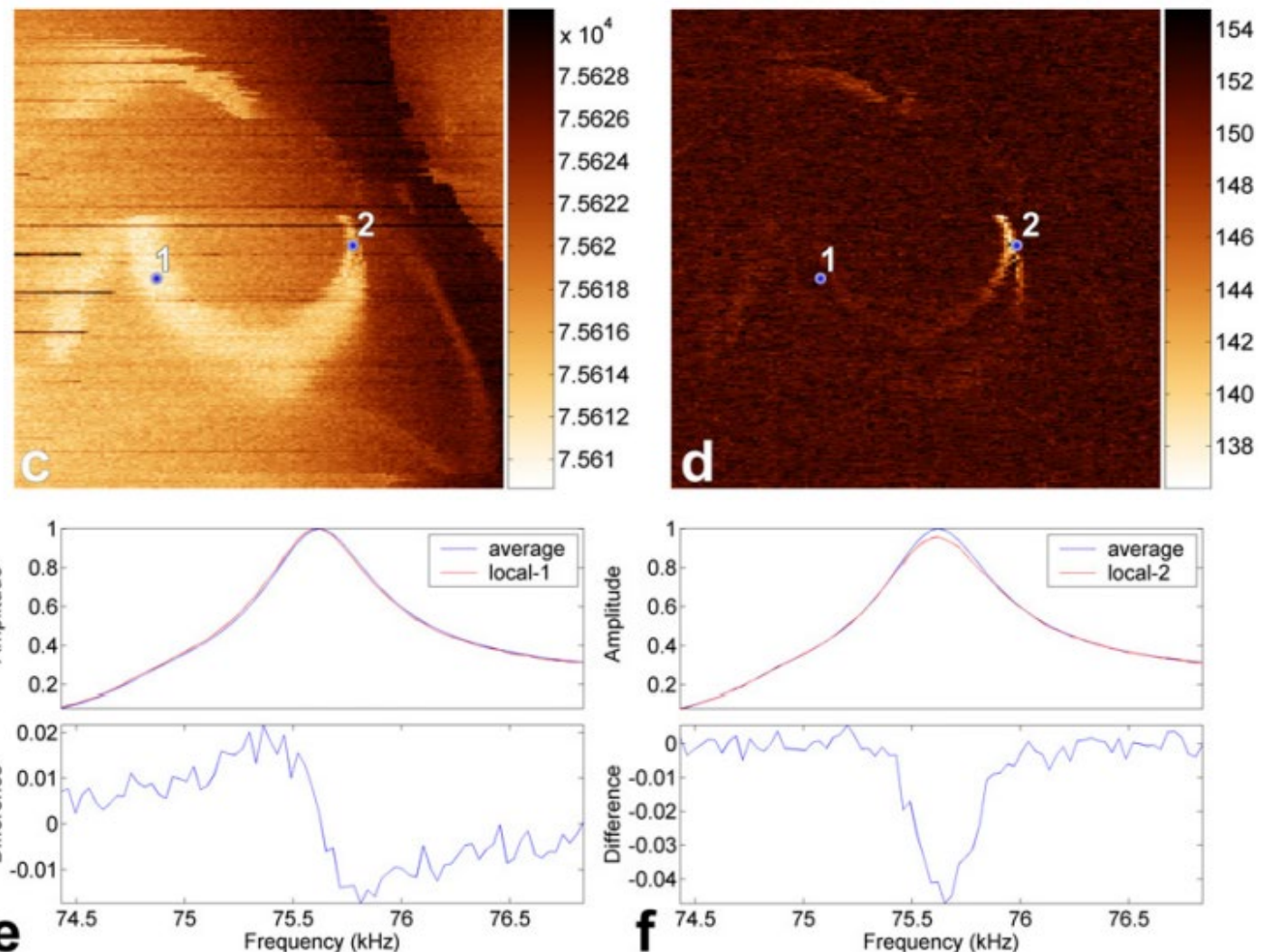
Spatial correlations

# Comparison: PCA vs. functional fit

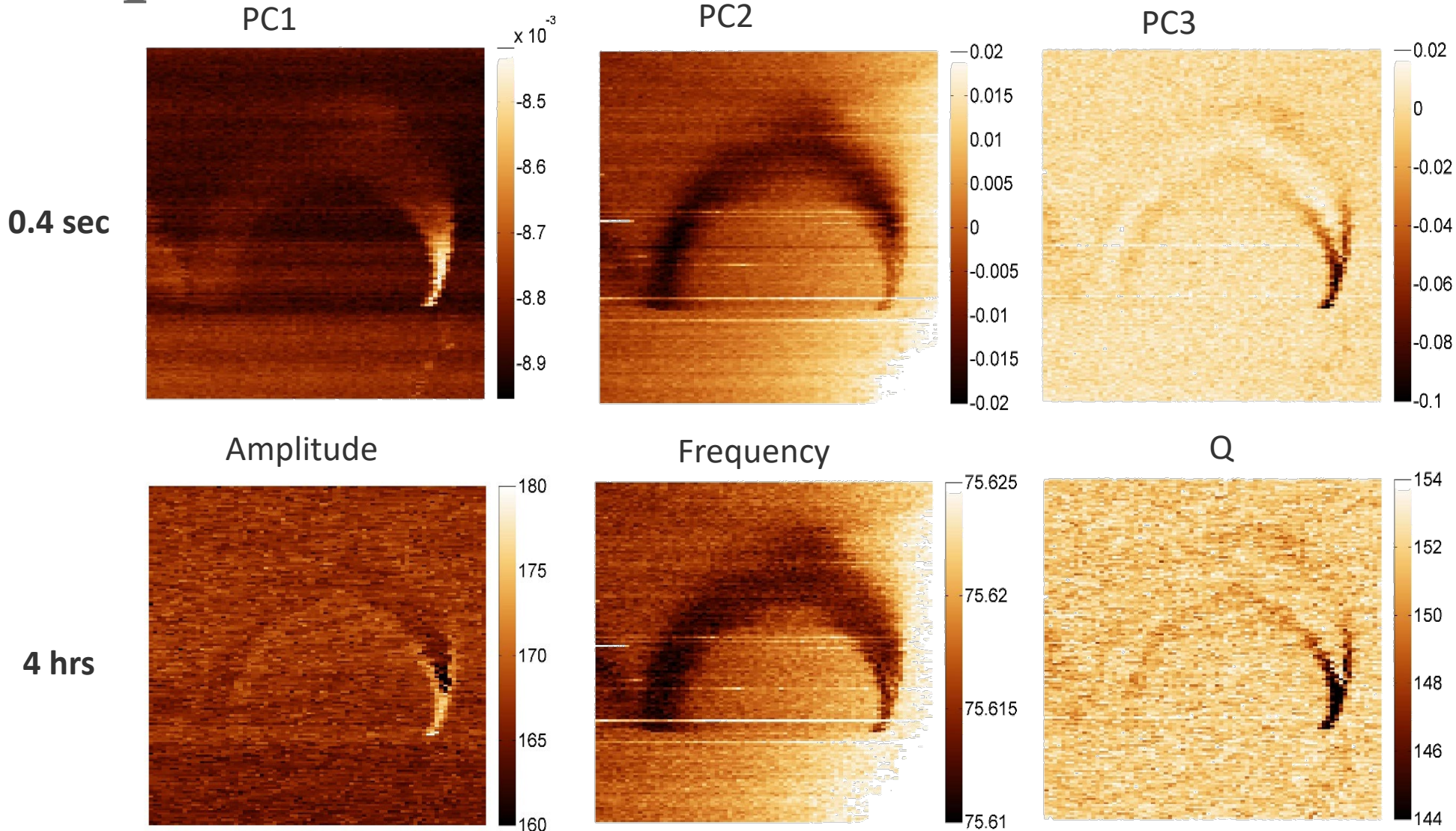
- Band excitation scanning probe microscopy
- Signal formation mechanism: simple harmonic oscillator

$$A(\omega) = \frac{A^{\max} \omega_0^2}{\sqrt{(\omega^2 - \omega_0^2)^2 + (\omega \omega_0 / Q)^2}}$$

$$\tan(\varphi(\omega)) = \frac{\omega \omega_0 / Q}{\omega^2 - \omega_0^2}.$$



# Comparison: PCA vs. functional fit

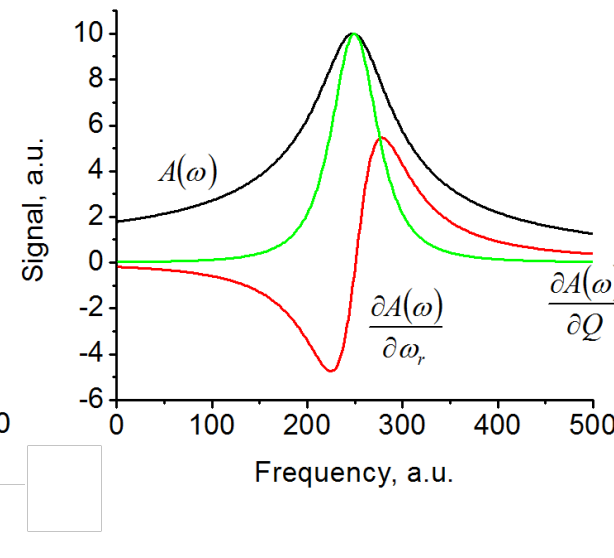
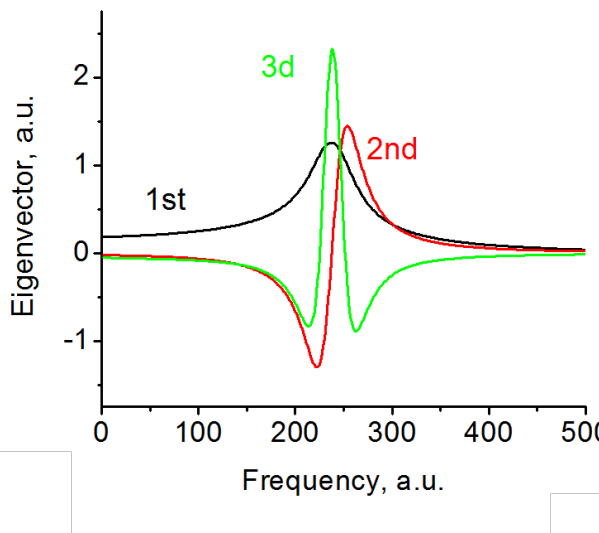
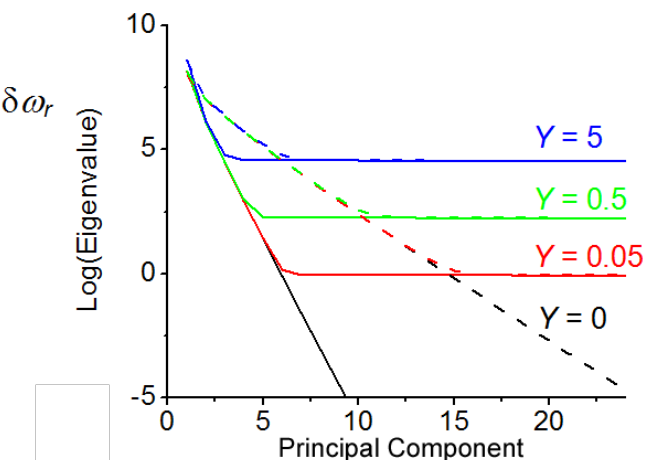
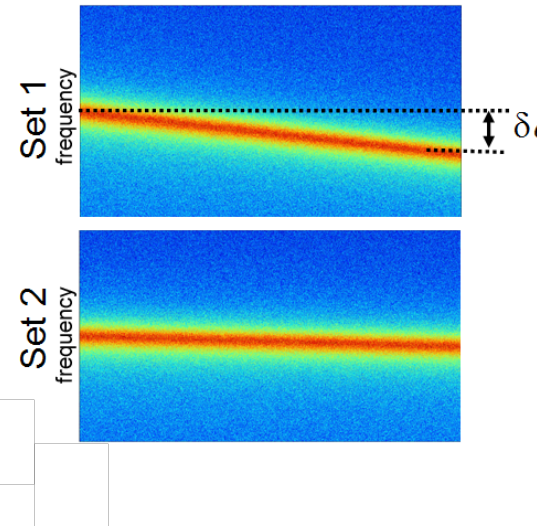


S. JESSE and S.V. KALININ, *Principal component and spatial correlation analysis of spectroscopic imaging data in scanning probe microscopy*, Nanotechnology **20**, 085714 (2009).

# When does PCA match physics?

Simulate simple harmonic oscillator curves for different variations of resonance frequency and noise levels

$$A(\omega) = \frac{F\omega\omega_r}{\sqrt{(\omega^2 - \omega_r^2)^2 + (\omega\omega_r/Q)^2}} + Y(\omega)$$



There is similarity between variational derivatives of SHO responses and PCA eigenvectors

$$\delta A_i(\omega) = \frac{\partial A(\omega)}{\partial F} \delta F_i + \frac{\partial A(\omega)}{\partial \omega_r} \delta \omega_{r,i} + \frac{\partial A(\omega)}{\partial Q} \delta Q_i + Y(\omega)$$

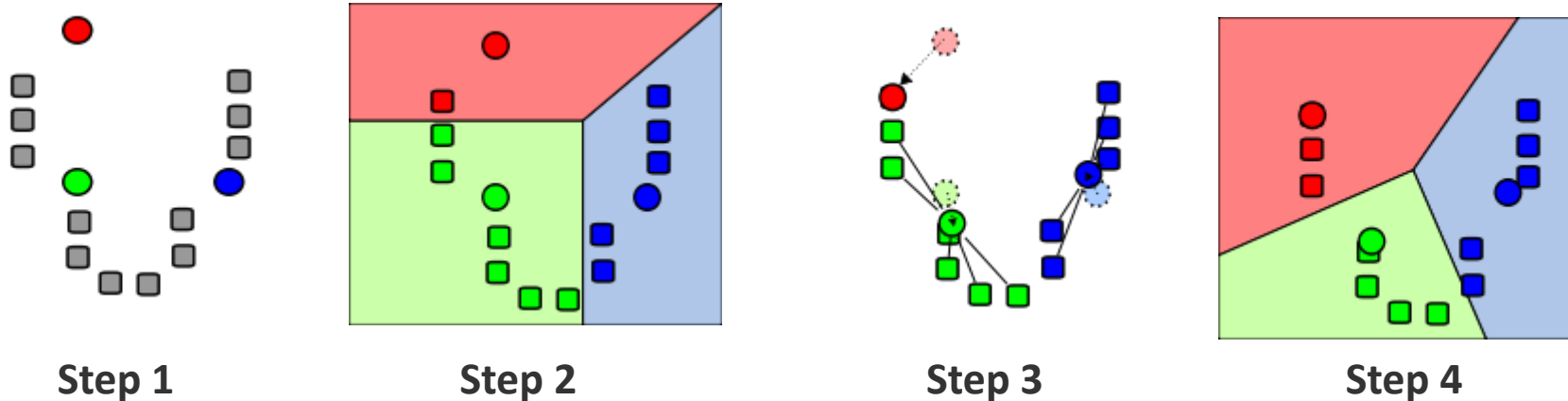
# K-mean clustering

- PCA is decomposition. But sometimes, we don't want to decompose our signal, but just group them in 'alike' sets.
- This is termed 'clustering'. The easiest and most widely used method is the k-means algorithm

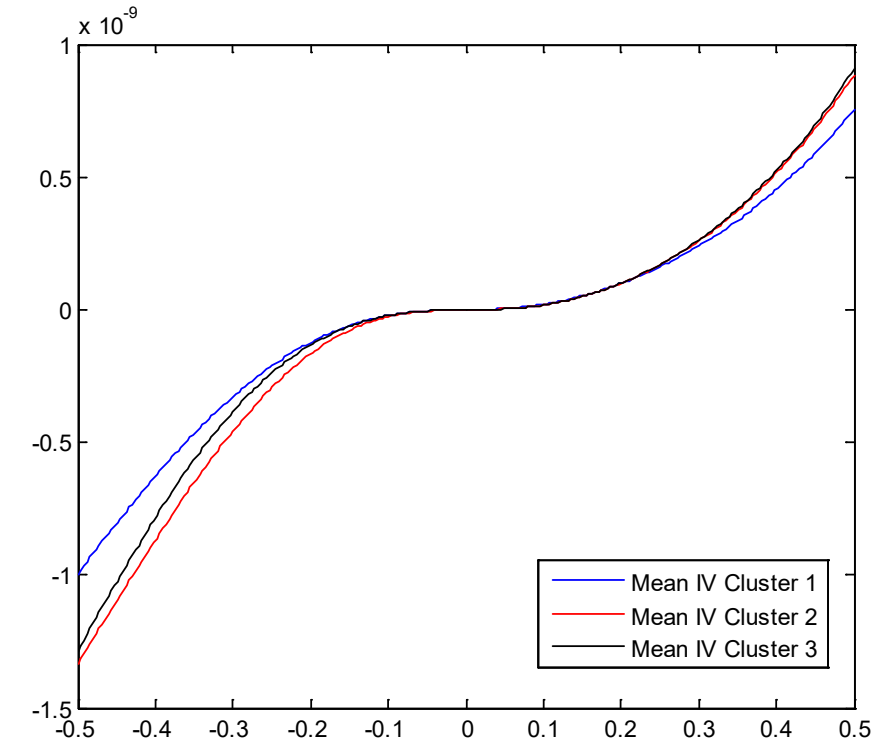
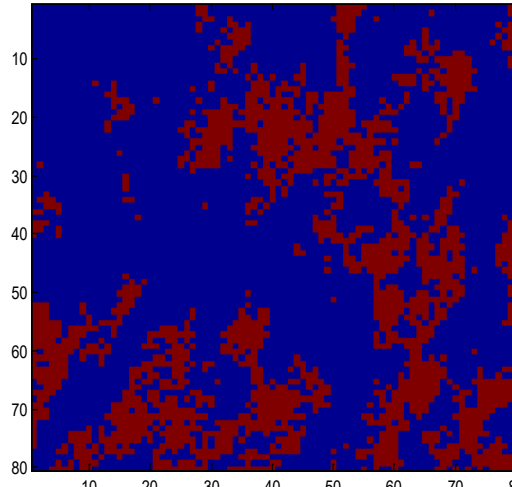
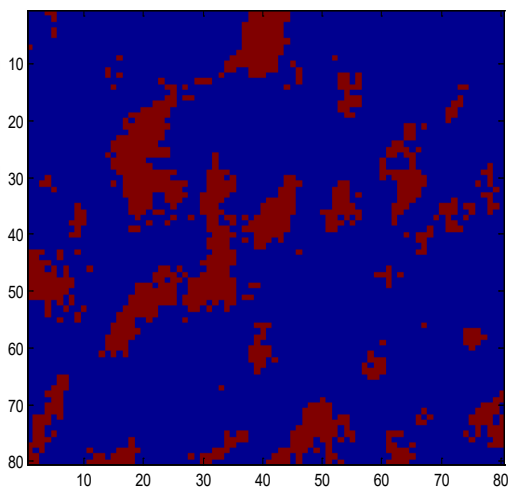
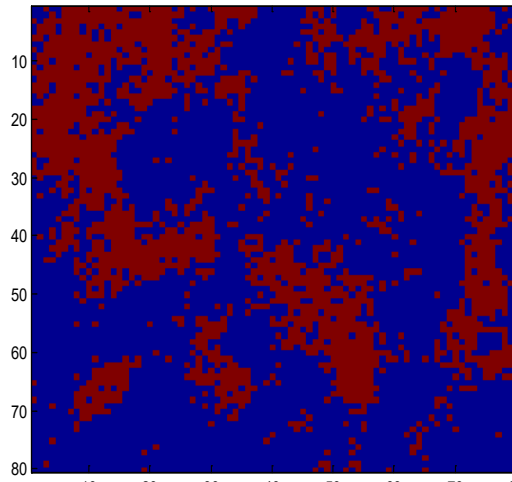
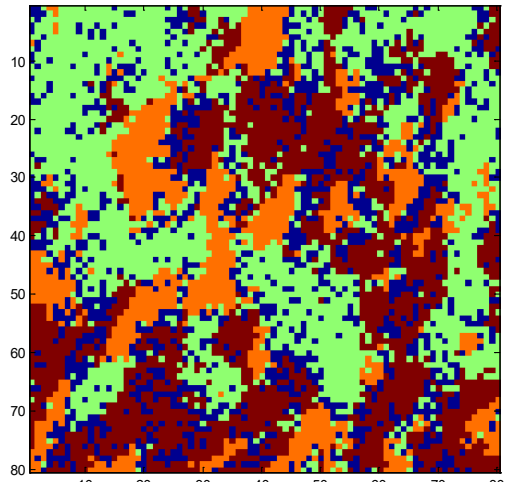
**K-means Clustering algorithm, to separate data ( $x_1, x_2, \dots, x_n$ ) into  $k$  clusters**

$$\arg \min_s \sum_{i=1}^k \sum_{x \in S_i} \|x - \mu_i\|^2 \quad \text{where } \mu_i \text{ is the mean of points in } S_i$$

(Determine  $S = \{S_1, S_2, \dots, S_k\}$ , such that within cluster sum of squares is minimized)



# K-means clustering



M. ZIATDINOV, A. MAKSOV, L. LI, A. SEFAT, P. MAKSYMOVYCH, and S.V. KALININ, *Deep data mining in a real space: Separation of intertwined electronic responses in a lightly-doped BaFe<sub>2</sub>As<sub>2</sub>*, Nanotechnology **27**, 475706 (2016).

K-means result of the CITS map broken into three distinct clusters: CITS map of all three clusters combined vs. individual cluster distribution in the map

# Independent Component Analysis

- **PCA:** orthogonal transformation of possibly correlated variable into a set of linearly uncorrelated variables
  - Analyzes data representing observations described by dependent variables which are inter-correlated
  - Main goal is to find true variables assuming that corrupting noise is Gaussian
- **ICA:** method for separating multivariate signal into additive subcomponents assuming statistical independence of source signals
  - Finds components that are maximally independent and non-Gaussian
  - Blind source separation – cocktail party problem

Compared to PCA, ICA can produce statistically independent non-Gaussian components by decorrelating the higher-order moments in addition to the first- and second-order moments of the statistical distribution

# Mathematics of ICA

**The Goal** is to transform observed data into maximally independent components measured through some function  $F(s_1, \dots, s_n)$  of independence.

- Data as a set of vectors  $\longrightarrow x = (x_1, \dots, x_m)^T$
- Components of the data  $\longrightarrow s = (s_1, \dots, s_n)^T$ .

$$s = Wx$$

An observed data vector  $x$  can then be represented as a sum of independent components  $s$  weighted by some mixing weight  $a$ :

$$x_i = a_{i,1}s_1 + \dots + a_{i,k}s_k + \dots + a_{i,n}s_n \quad \text{or} \quad x = \sum_{k=1}^n s_k a_k$$

In other words, data vector  $x$  is represented by basis vectors  $a_k = (a_{1,k}, \dots, a_{m,k})^T$  that can form columns of a mixing matrix such that:  $x = As$

# Mathematics of ICA - 2

$$x = As$$

Given that our data is set of vectors  $x$ , we want to find both, the mixing matrix  $A$  and sources  $s$

This can be done by calculating  $w$  vectors and a cost function that can maximize the Non-Gaussianity, or minimize mutual information of

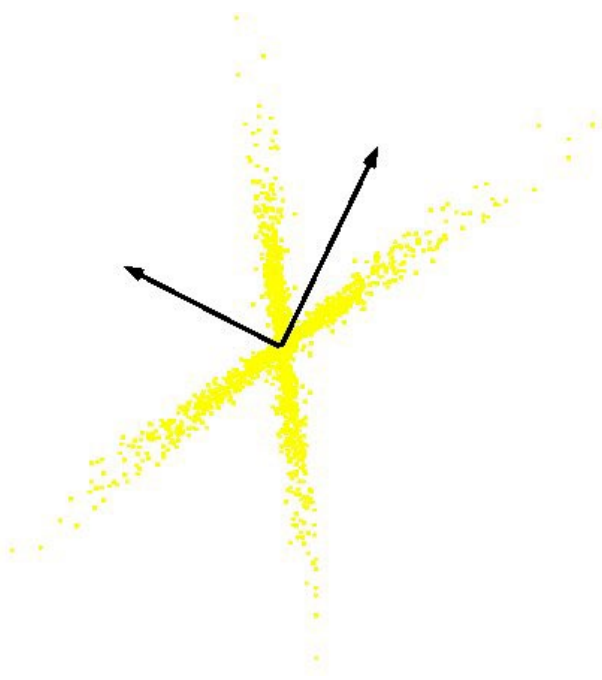
$$s_k = (w^T * x)$$

Original sources can then be recovered by multiplying observed data vectors  $x$  with the inverse of the mixing matrix:  $W = A^{-1}$

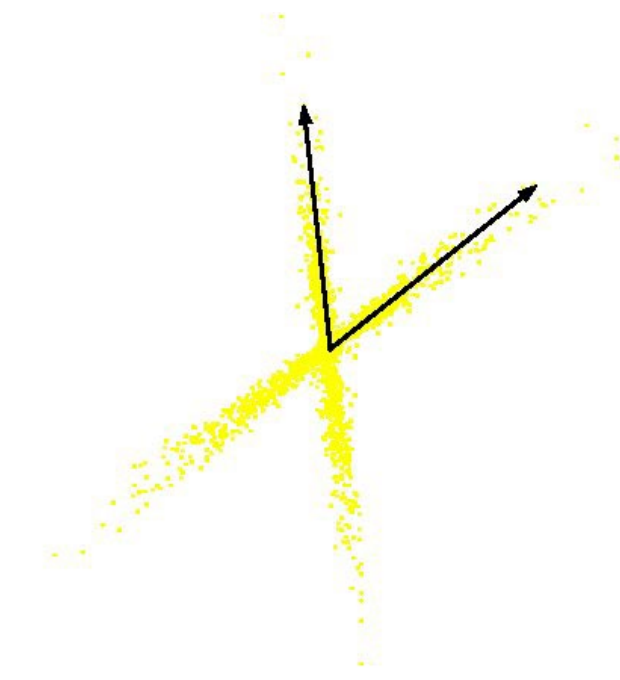
- Not as easy to utilize as PCA, but excellent premade algorithms are readily available, e.g. Aapo Hyvärinen – FastICA\*

[http://cis.legacy.ics.tkk.fi/aapo/papers/IJCNN99\\_tutorialweb/IJCNN99\\_tutorial3.html](http://cis.legacy.ics.tkk.fi/aapo/papers/IJCNN99_tutorialweb/IJCNN99_tutorial3.html)  
<http://research.ics.aalto.fi/ica/fastica/>

# PCA vs. ICA

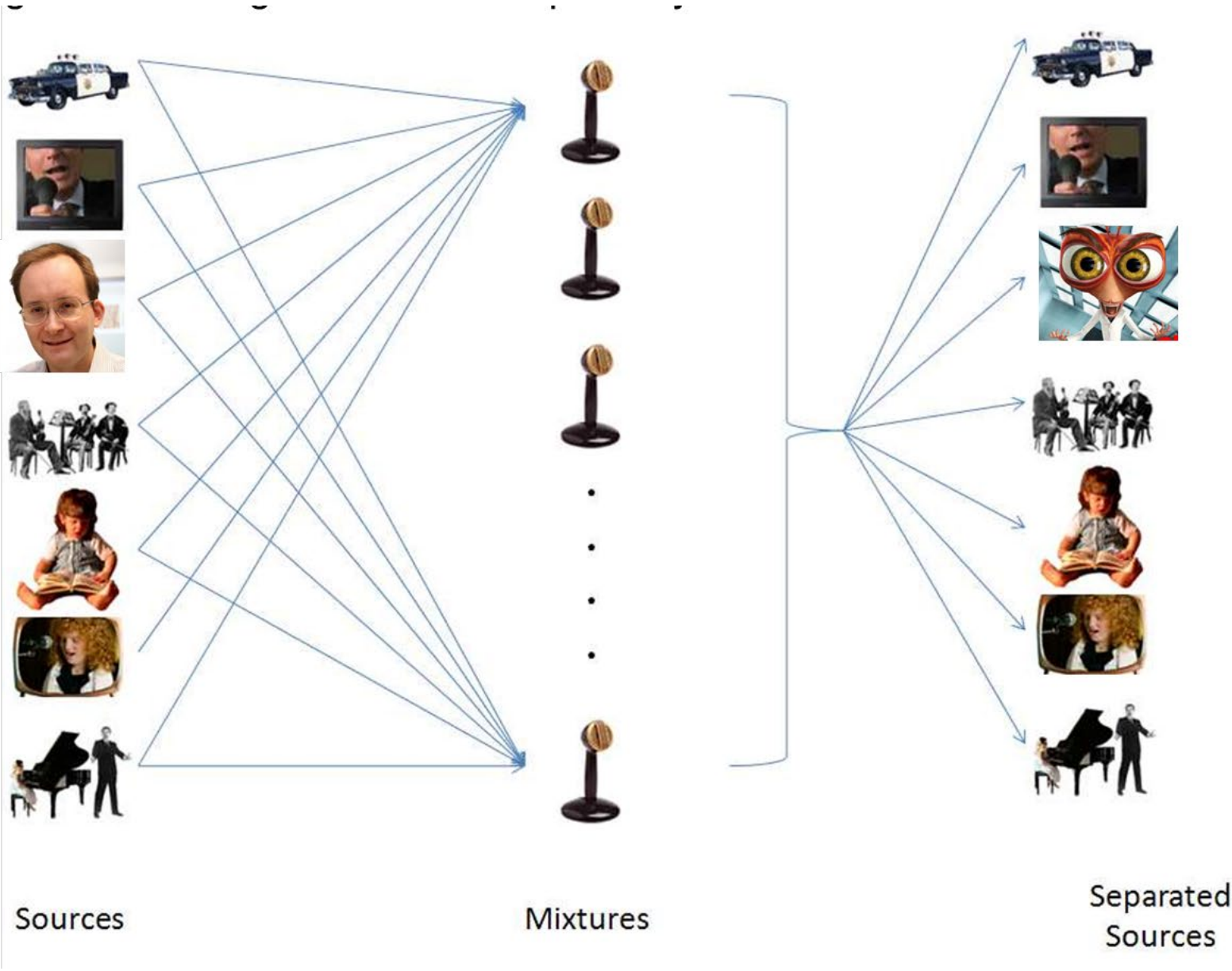


PCA  
(orthogonal coordinate)



ICA  
(non-orthogonal coordinate)

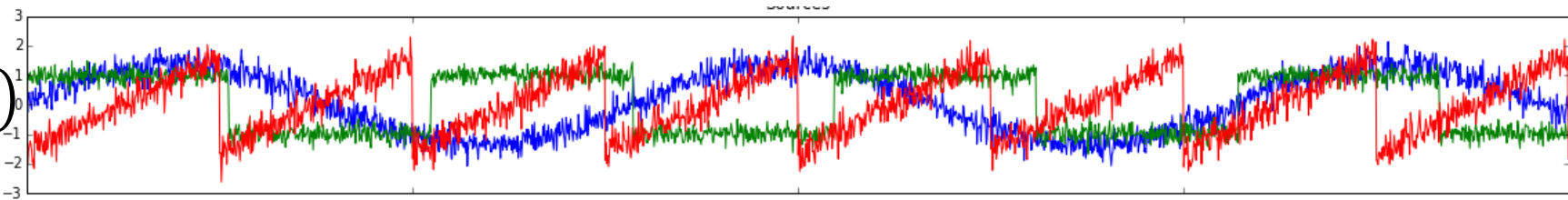
# Cocktail Party Problem



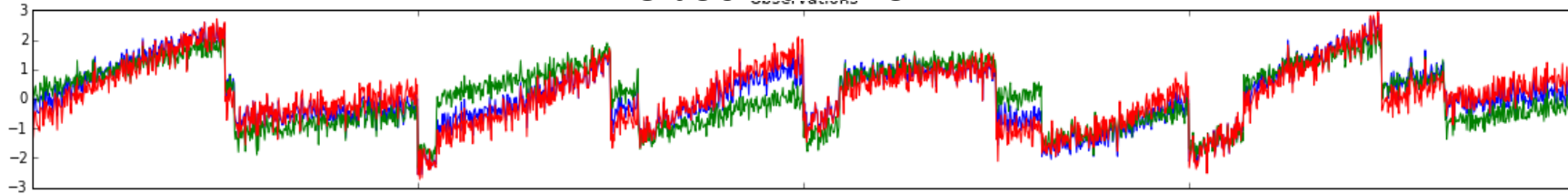
# ICA Example

$$(R_1(t), R_2(t), \dots, R_n(t))$$

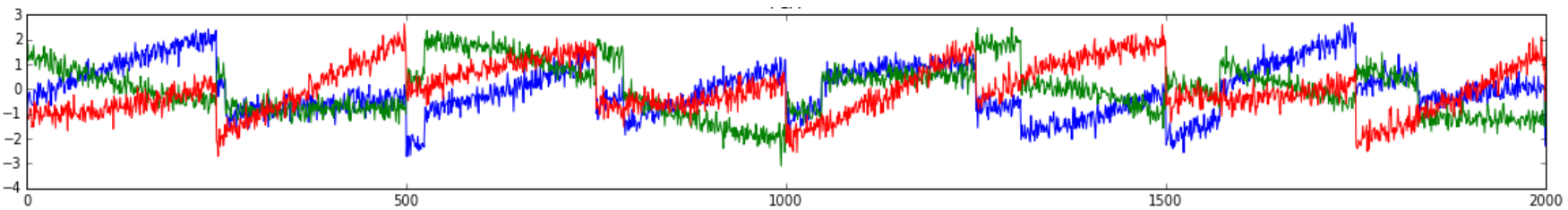
Sources



Observations



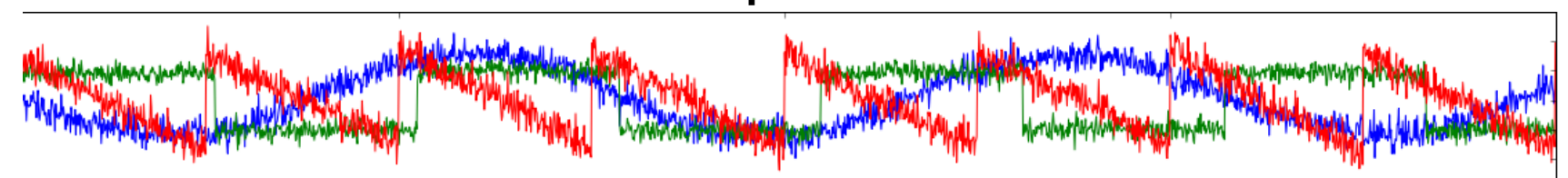
PCA Components



Components are  
maximally independent

ICA Components

$$\begin{pmatrix} R_1(t) \\ \dots \\ R_n(t) \end{pmatrix} = A \begin{pmatrix} s_1(t) \\ \dots \\ s_n(t) \end{pmatrix}$$

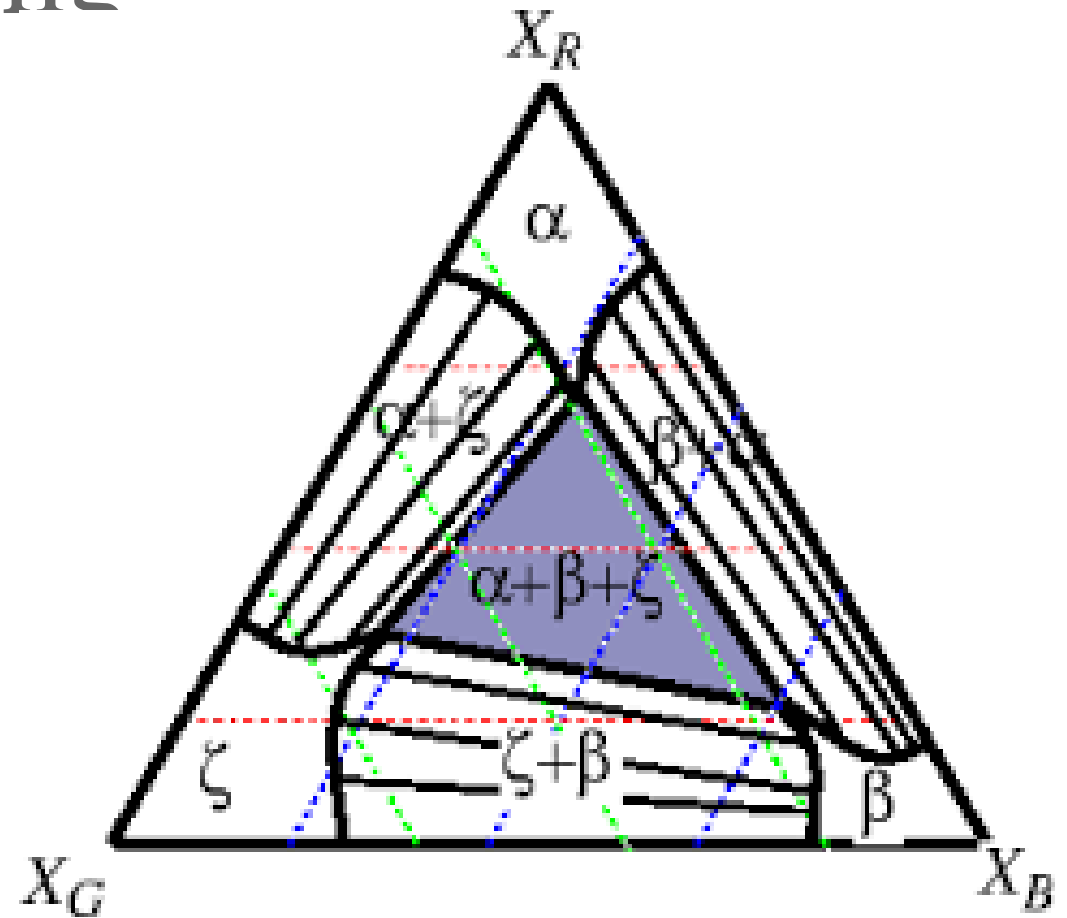


# Bayesian Linear Unmixing

$$S(\mathbf{x}, \mathbf{R}) = \sum_{i=1}^K a_i(\mathbf{x}) w_i(\mathbf{R}) + \mathbf{N}$$

$$\sum_{i=1}^K a_i(\mathbf{x}) = 1$$

- The eigenvectors  $w_i(\mathbf{R})$  are non-negative,  $w_i(\mathbf{R}) \geq 0$
- The loading coefficients sum to 1
- The number of eigenvectors,  $K$ , is a priori unknown

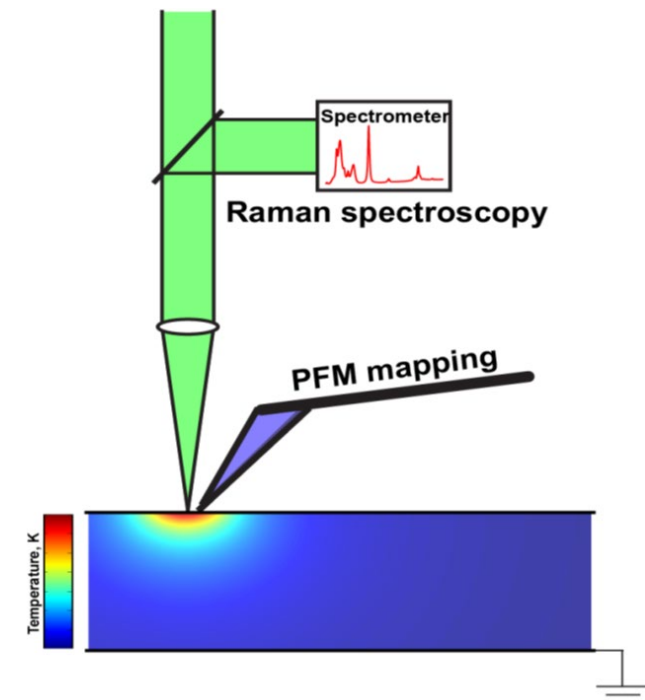


BLU is ideally suited for certain classes of problems, e.g. conduction through parallel channels, optical or electronic spectra of mixtures, etc

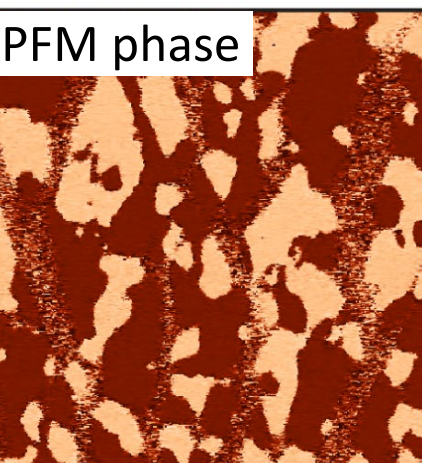
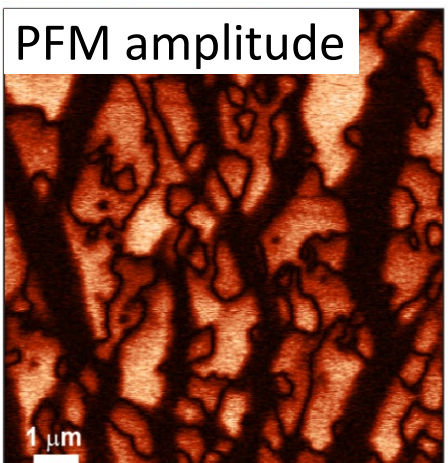
# Laser heating induced phase transitions

- Copper indium thiophosphate ( $\text{Cu}_{0.77}\text{In}_{1.12}\text{P}_2\text{S}_6$ ) layered ferroelectric
  - Ferroelectric state at room temperature
  - Curie temperature  $T_c = 320$  K
  - Non-polar  $\text{In}_{4/3}\text{P}_2\text{S}_6$  inclusions
- Combined Atomic Force Microscopy (AFM) and confocal Raman spectroscopy investigative approach
  - AFM – topography measurements
  - Piezoresponse force microscopy (PFM) – static ferroelectric domain structure
  - Raman – crystallographic structure via Raman spectra

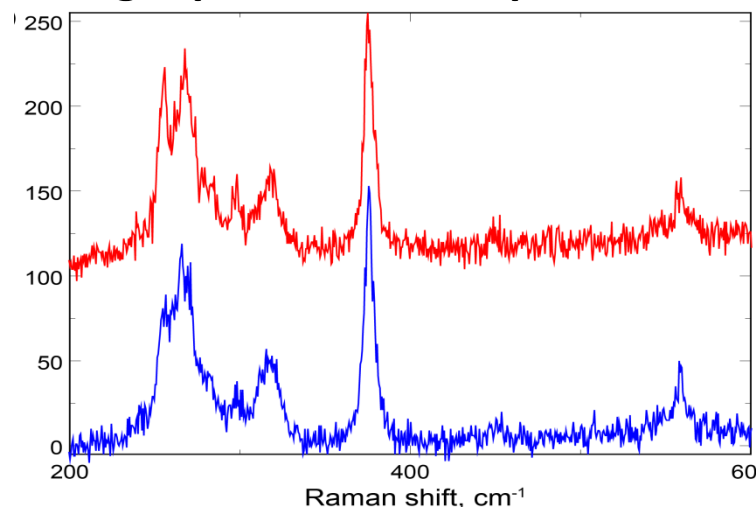
## Experimental scheme



Ferroelectric domain structure



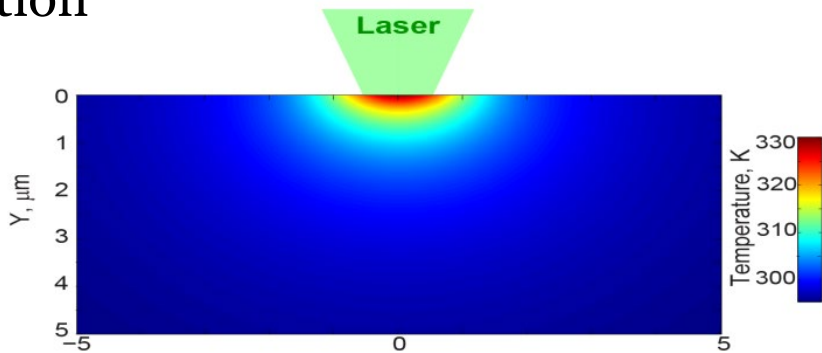
Single point Raman spectra



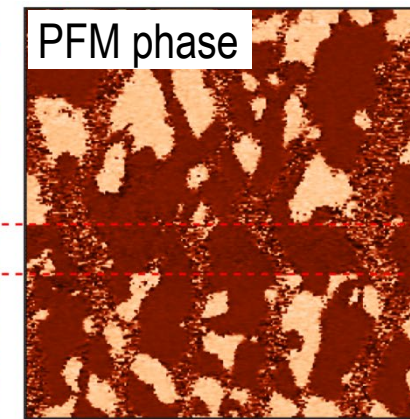
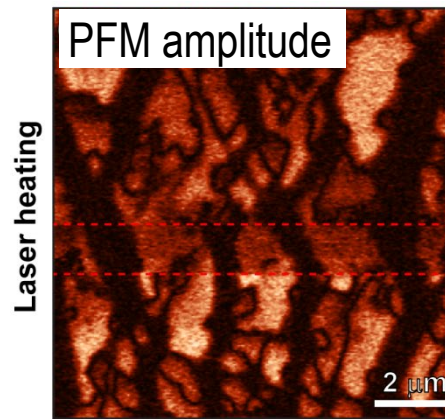
A. ILEV, ACS Nano  
9, 12442 (2015).

# Laser heating induced phase transition

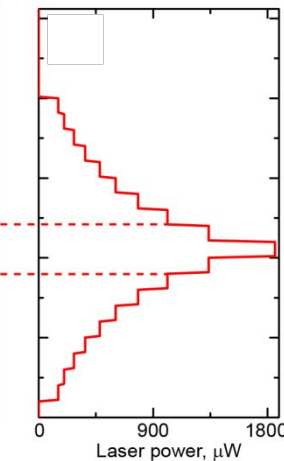
Laser can be used for local heating to induce ferroelectric- paraelectric phase transition



Domain structure evolution

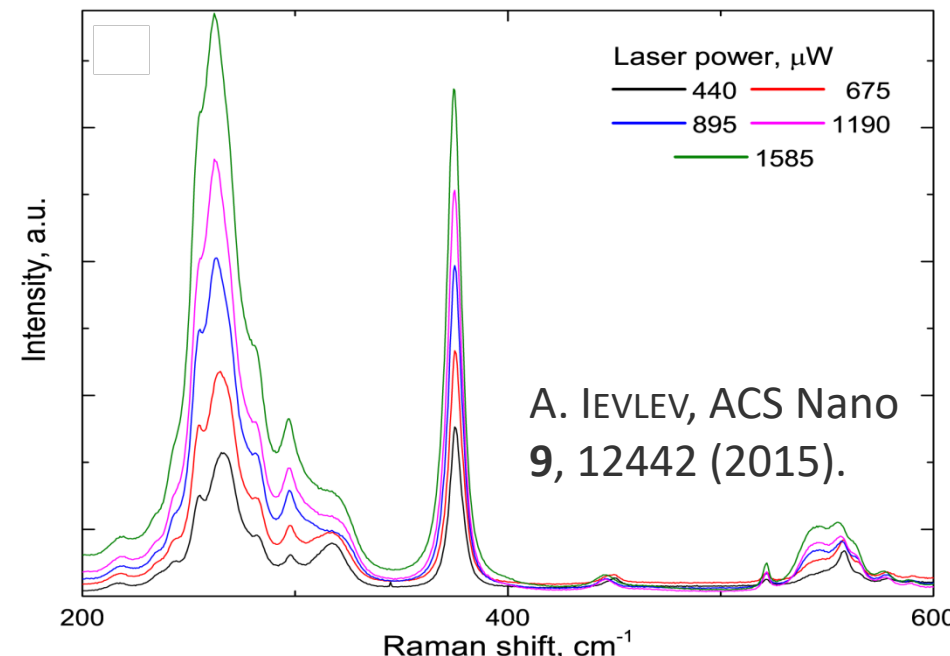


Laser power



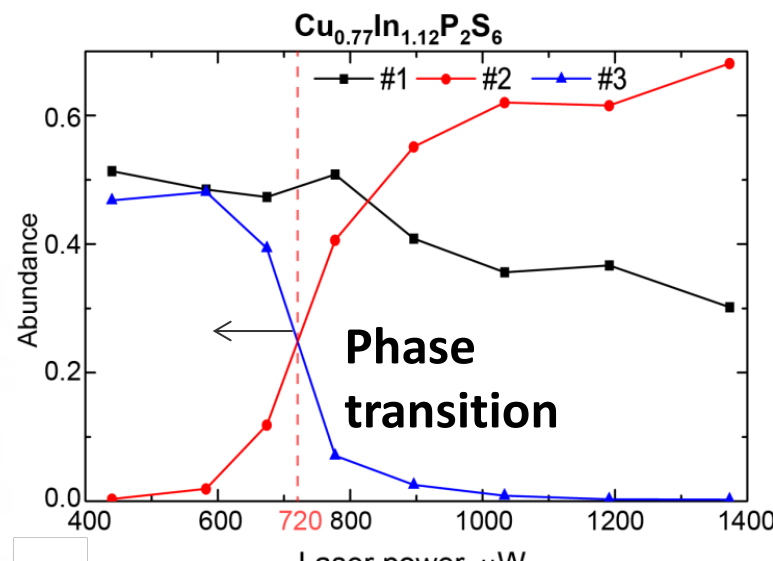
- Measurements with variation of the laser power
  - PFM – *in-situ* change in the domain structure above  $T_c$
  - Raman – evolution of the Raman spectra through the phase transition
- Comprehensive analysis of Raman spectra is complicated by inhomogeneous chemical composition and high noise level
- Bayesian Linear Unmixing can be used for automated identification of spectra evolution

Raman spectra evolution (averaged)



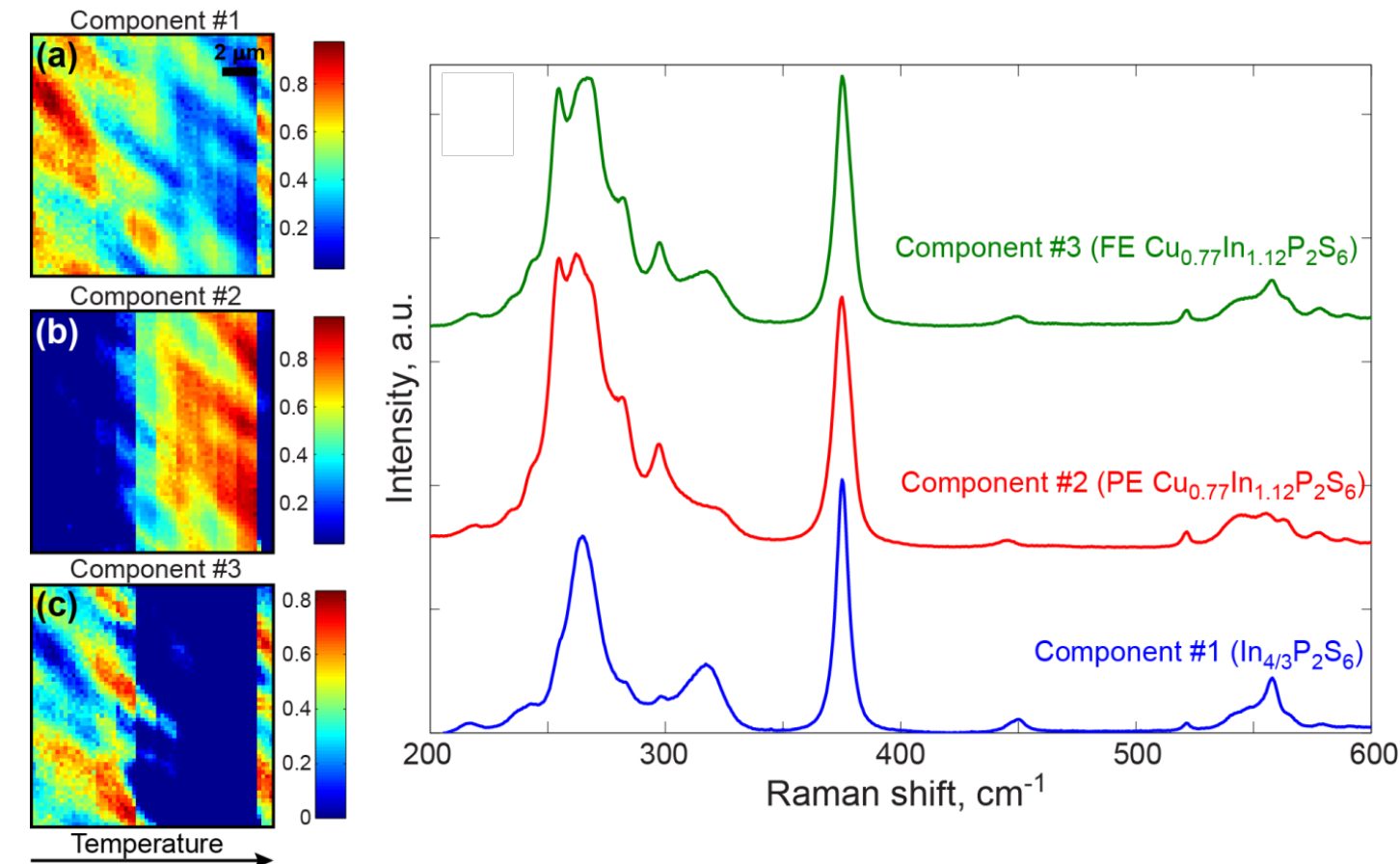
# BLU separation of components

Spatial concentration of components



A. Ievlev, ACS Nano 9, 12442 (2015).

Results of BLU: components and loading maps

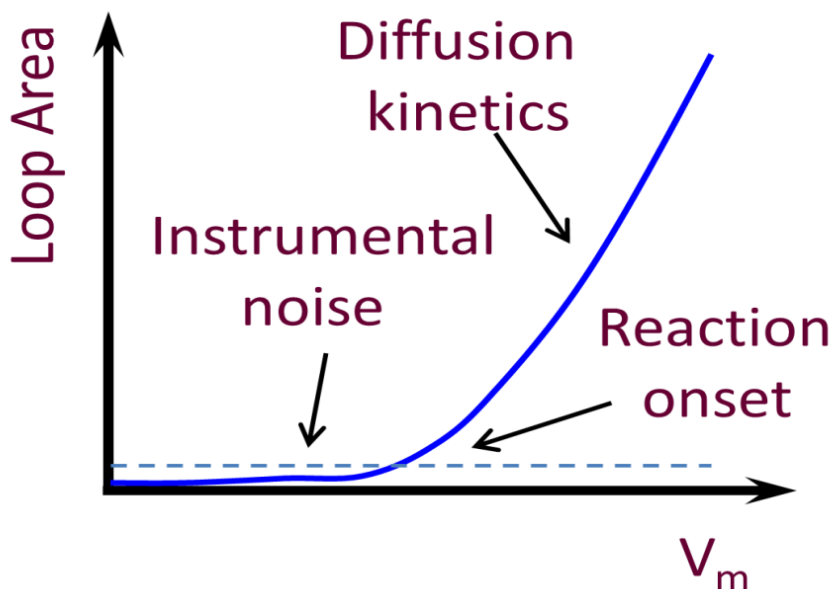
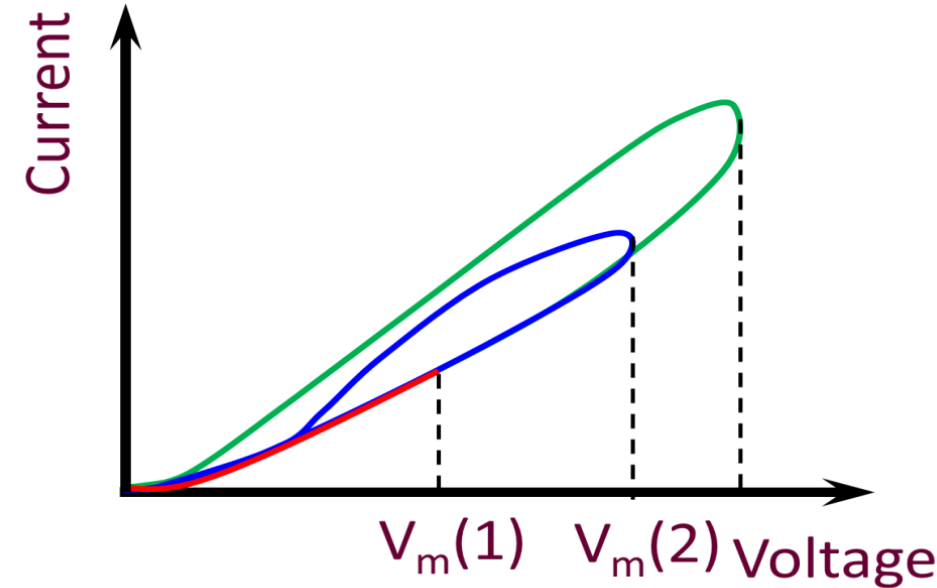
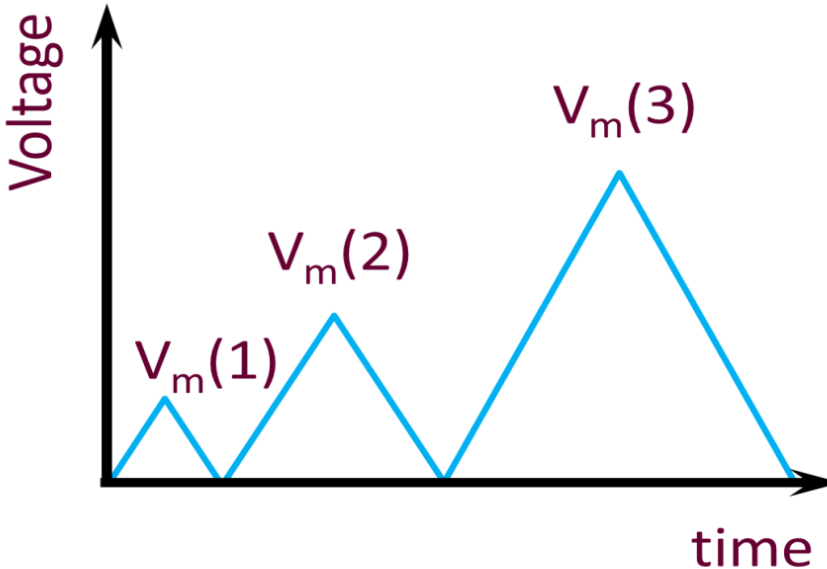


Unmixing showed presence of three independent components in Raman spectra:

1. Non-polar  $\text{In}_{4/3}\text{P}_2\text{S}_6$  – weak changes in intensity with temperature
2. Paraelectric  $\text{CuInP}_2\text{S}_6$  above  $T_c$  – appears at higher laser powers
3. Ferroelectric  $\text{CuInP}_2\text{S}_6$  below  $T_c$  – disappears at higher temperatures

# Notebook

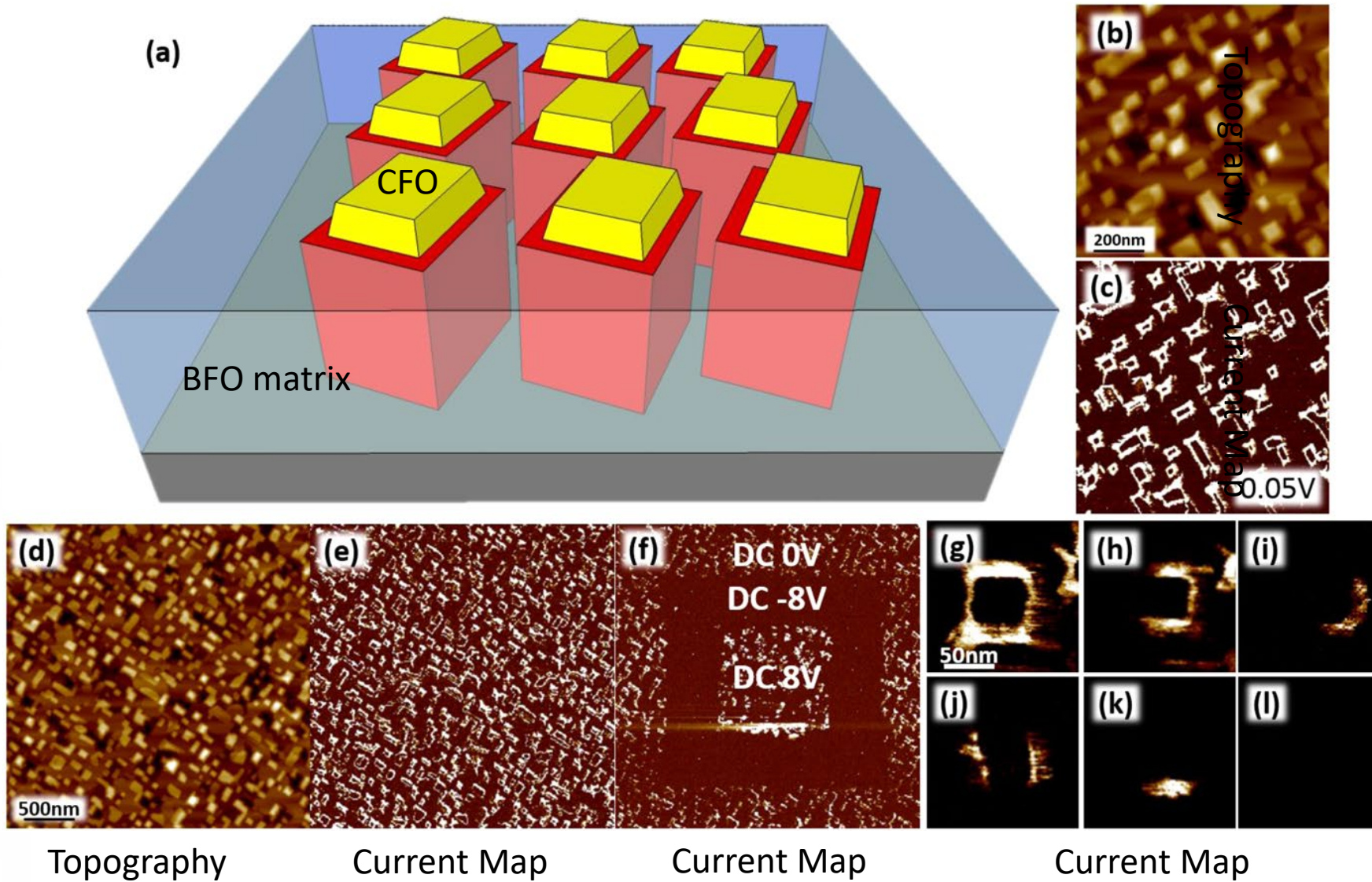
# First order reversal curve IV measurements



- First order reversal curves in IV measurements
- Opening of hysteresis loops indicates onset of slow-bias-induced changes
- These can be explored as a function of rate and bias

# Conductance in nanotubular structures

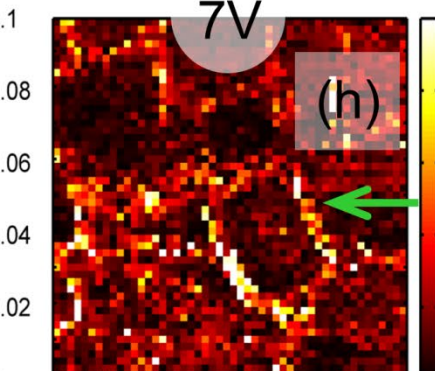
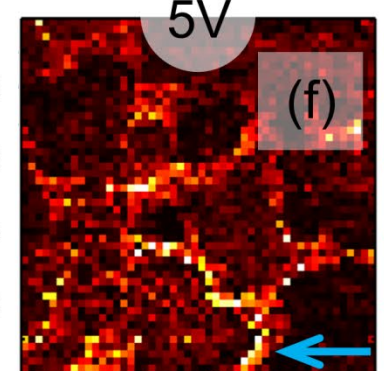
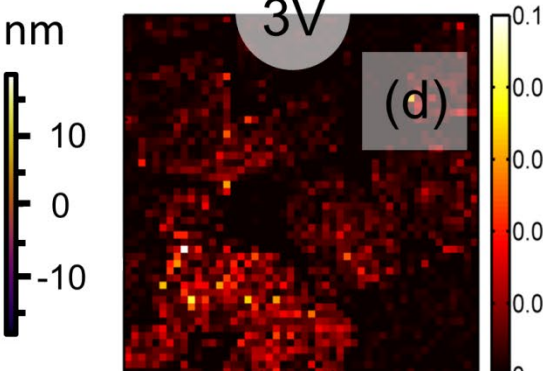
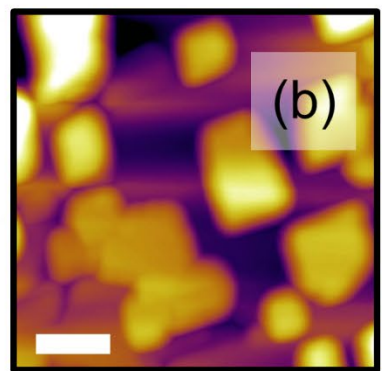
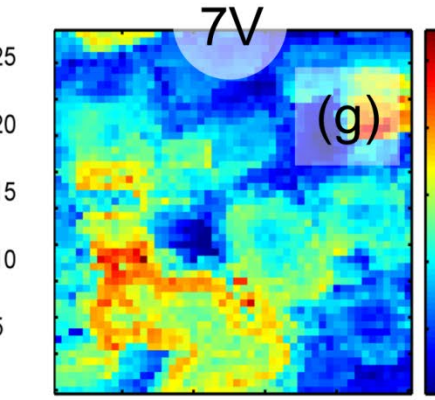
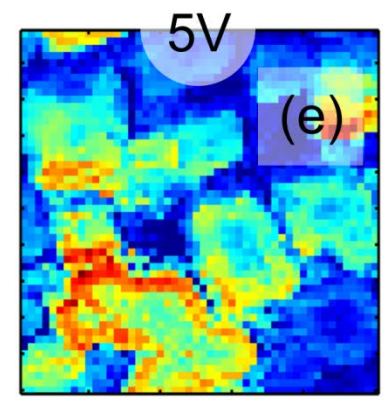
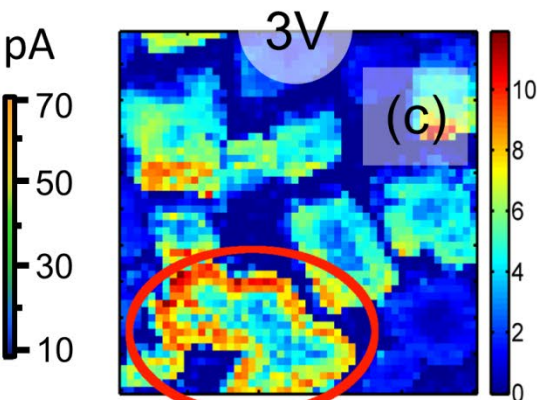
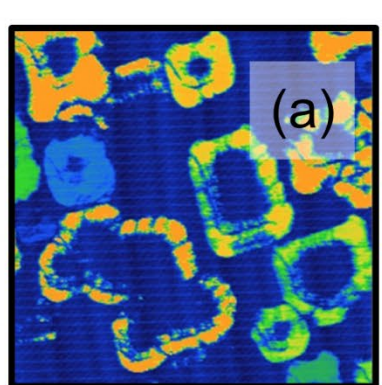
## Probing electrochemistry through electronic degrees of freedom



Y.H. HSIEH, E. STRELCOV, J.M. LIOU, C.Y. SHEN, Y.C. CHEN, S.V. KALININ, and Y.H. CHU, *Electrical Modulation of the Local Conduction at Oxide Tubular Interfaces*, ACS Nano 7, 8627 (2013).

# FORC IV of BFO-CFO

Current map @ 0.1 V

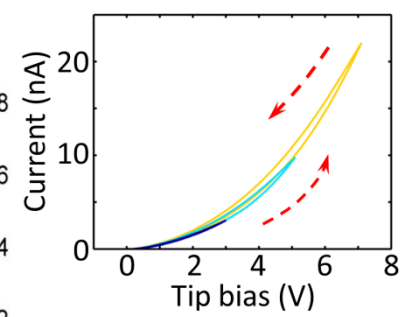
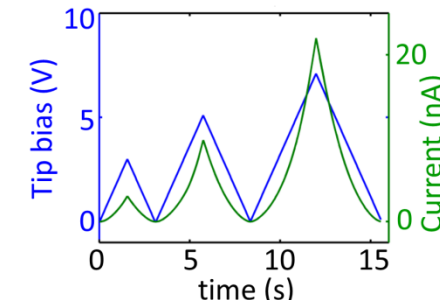


Topography

FORC-IV Loop area maps

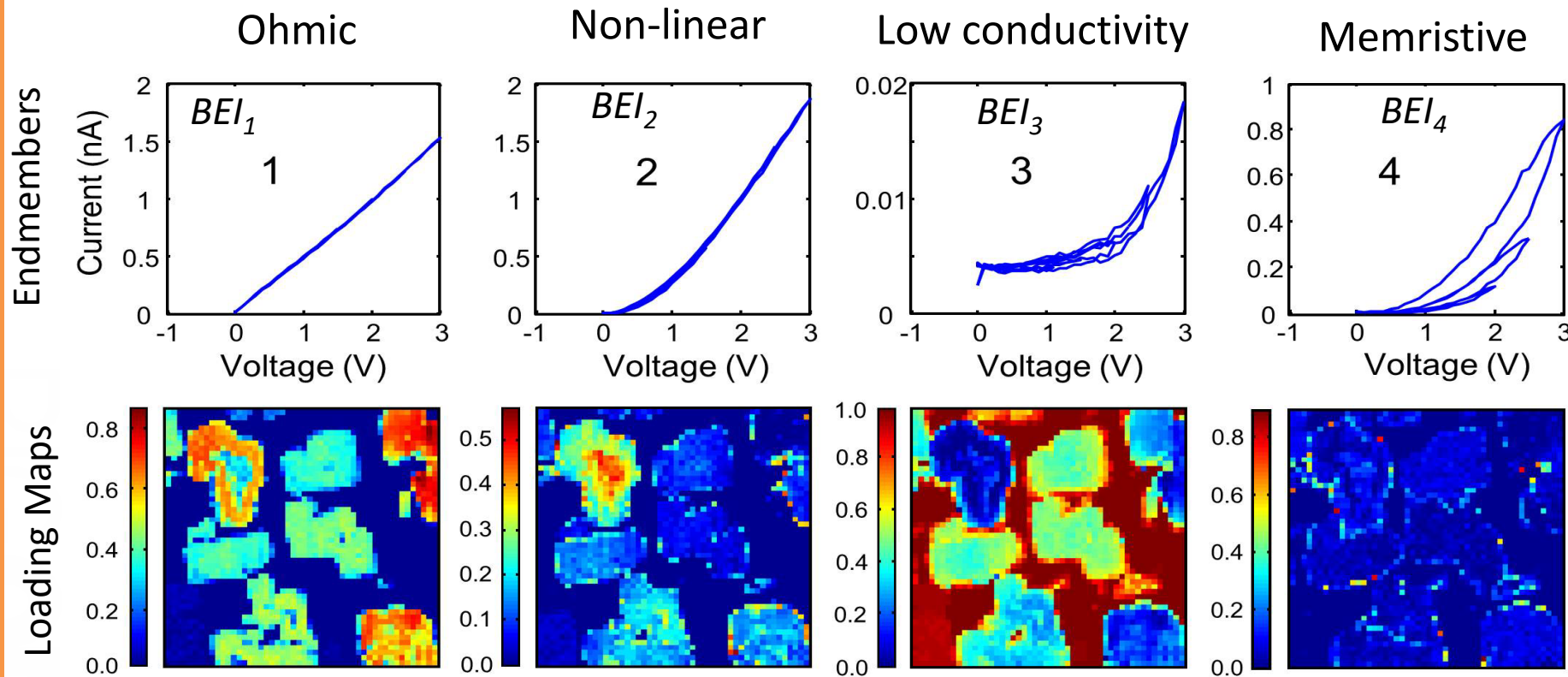
Current maps

Averaged IV's



- Clear variability of conductance and loop opening behavior
- “Too much data” – FORC IV loops that can be reduced to multiple current and loop opening maps as a function of peak voltage

# Bayesian linear unmixing



Separates 4 different types of behavior, all making physical sense. Loading maps normalized to unity.

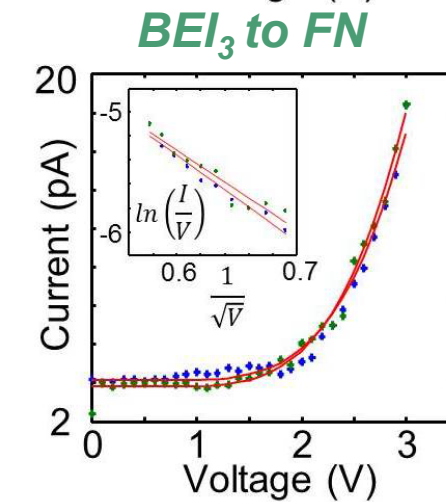
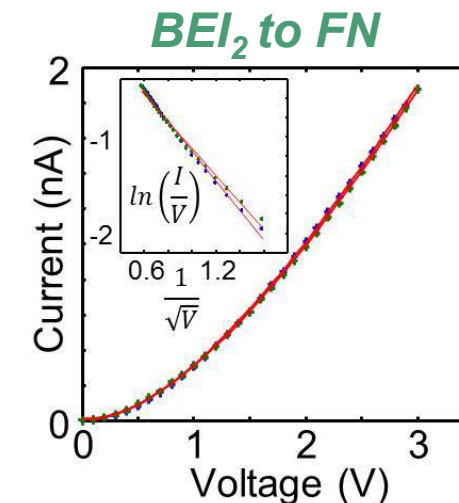
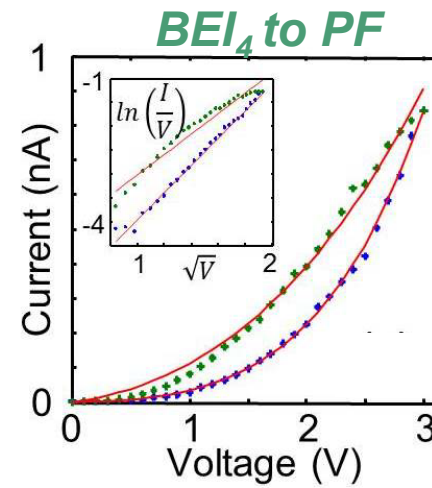
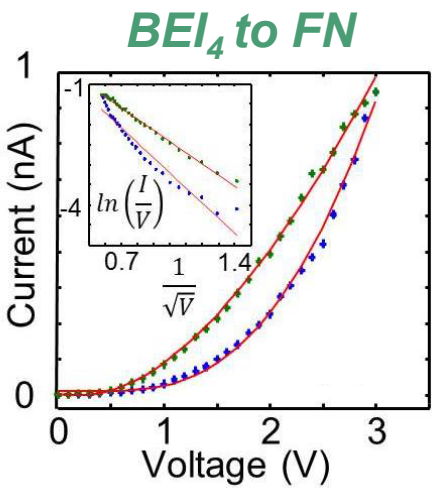
$$I_{xy} = \sum_j^n I_{xyj} = \sum_j^n \alpha_{xyj} BEI_j \quad \sum_j^n \alpha_{xyj} = 1$$

E. STRELCOV, A. BELIANINOV, Y.H. HSIEH, S. JESSE, A.P. BADDORF, Y.H. CHU, and S.V. KALININ,  
*Deep Data Analysis of Conductive Phenomena on Complex Oxide Interfaces: Physics from Data Mining*, ACS Nano 8, 6449 (2014).

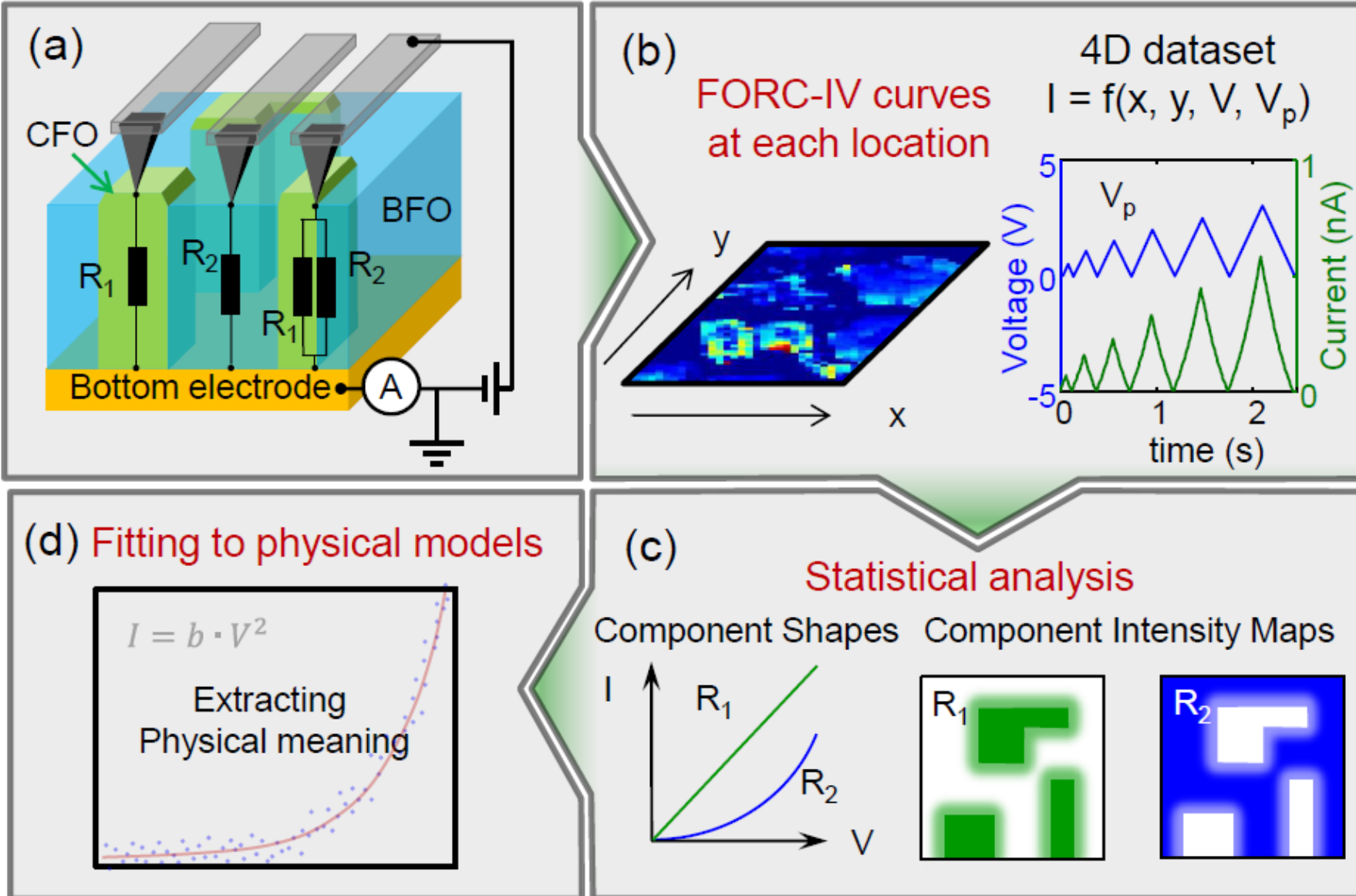
# Fit to physical models

Mechanism\Endmember	Fowler-Nordheim	Poole-Frenkel	Schottky	Mott-Gurney	Child's Law
1 <sup>st</sup>	-	-	-	-	-
2 <sup>nd</sup>	good <sup>†</sup>	bad	bad	good	good
3 <sup>rd</sup>	fair <sup>†</sup>	bad	bad	bad	bad
4 <sup>th</sup> forward	bad	good <sup>†</sup>	bad	bad	bad
4 <sup>th</sup> reverse	good <sup>†</sup>	bad	fair	bad	bad

<sup>†</sup>The values of the fitting coefficients are physically meaningful



# FORC IV workflow



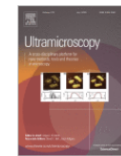
# Wait, there is more!

We need un-mixing/decomposition that are infused in some universal manner with a priori physical information (trivial example is constraints, a less trivial one is a simulation of some expected components) so that the resultant components can be directly interpreted in physical terms.

## **For example:**

- Bayesian linear unmixing: constraints on endmembers
- Sparse reconstructions: small number of components in each point
- Constraints on loading maps: smoothness or sharp boundaries
- Kernel transforms: data is simplest if physics is correct

# Neural Networks for Spectrum Analysis



Quantification

# Analyzing line scan EELS data with neural pattern recognition

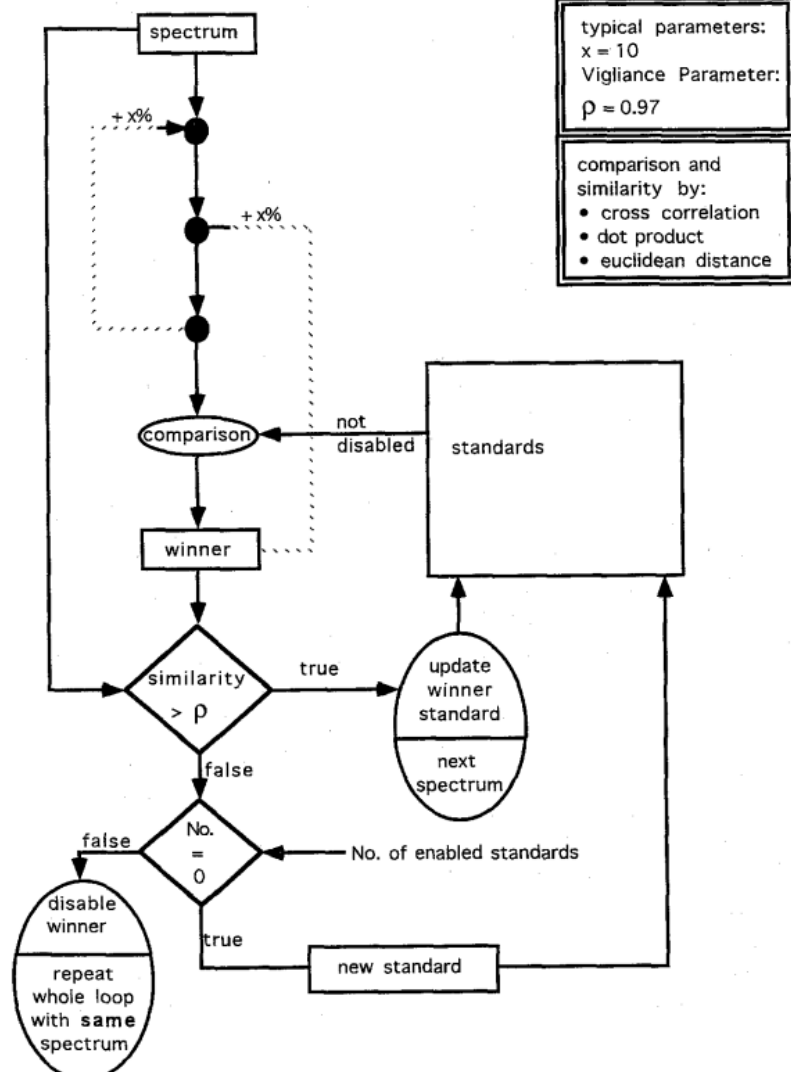
C. Gatts<sup>1</sup>, G. Duscher<sup>2</sup>, H. Müllejans, M. Rühle

Show more ▾

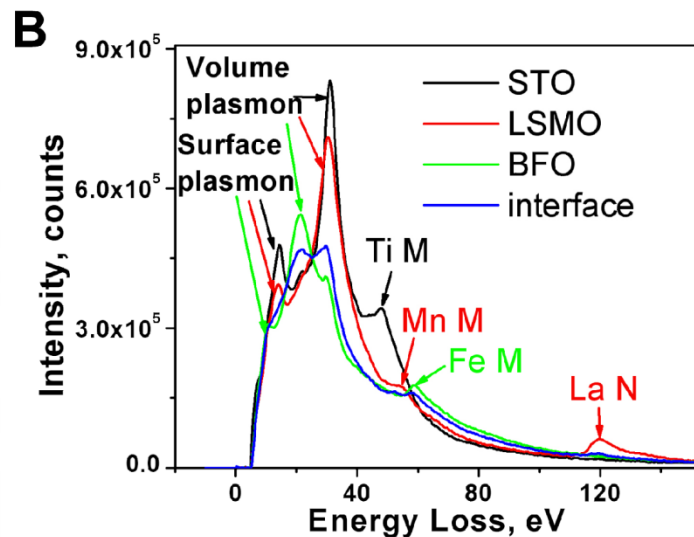
[+ Add to Mendeley](#) [Share](#) [Cite](#)[https://doi.org/10.1016/0304-3991\(95\)00031-U](https://doi.org/10.1016/0304-3991(95)00031-U)[Get rights and content](#)[Full text access](#)

## Abstract

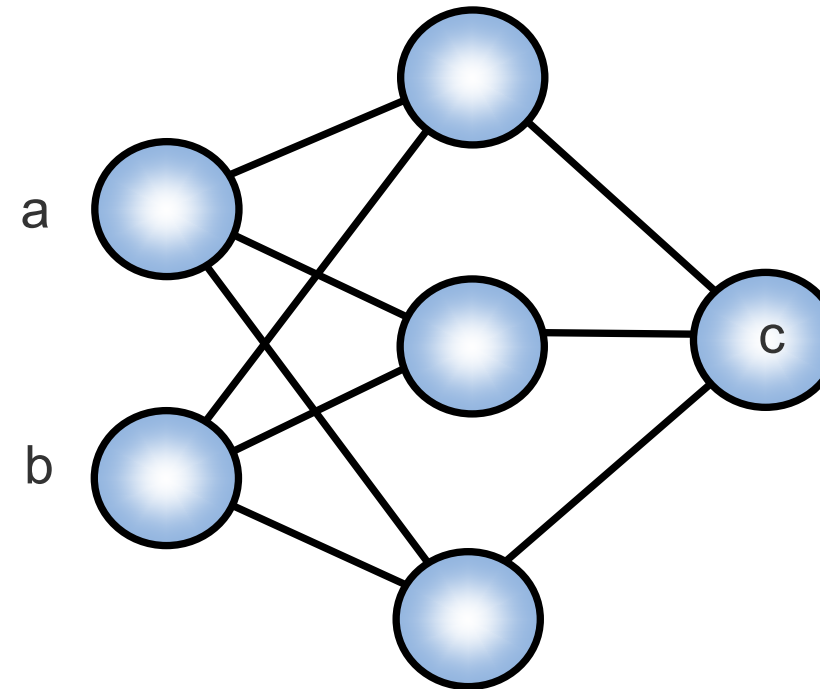
Neural Pattern Recognition was used for extracting chemical state information from electron energy-loss (EEL) spectra. The purpose was to obtain a quantitative composition profile from sets of low-loss and core-loss EEL spectra measured along a line across an amorphous inclusion at a grain boundary in a silicon bicrystal. The spectra were presented serially to the artificial neural network to obtain the number and shape of the spectra, whose linear combinations reproduce each single spectrum. The results indicate the existence of a different chemical environment at the interfaces between inclusion and crystal. The data analysis proved to be fast, robust, relatively immune to noise or artifacts and capable of extracting relevant information from subtle spectral features.



# Simple example: NN on EELS data



$a^*weight + bias$

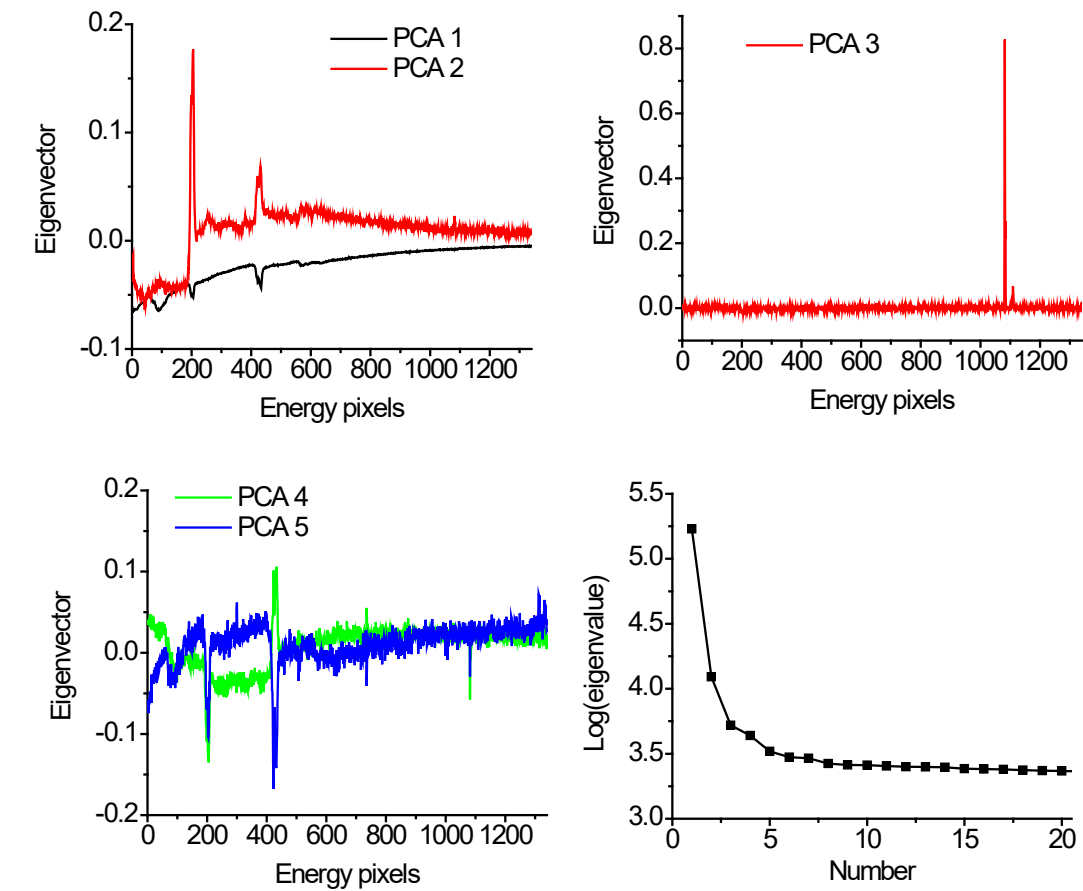
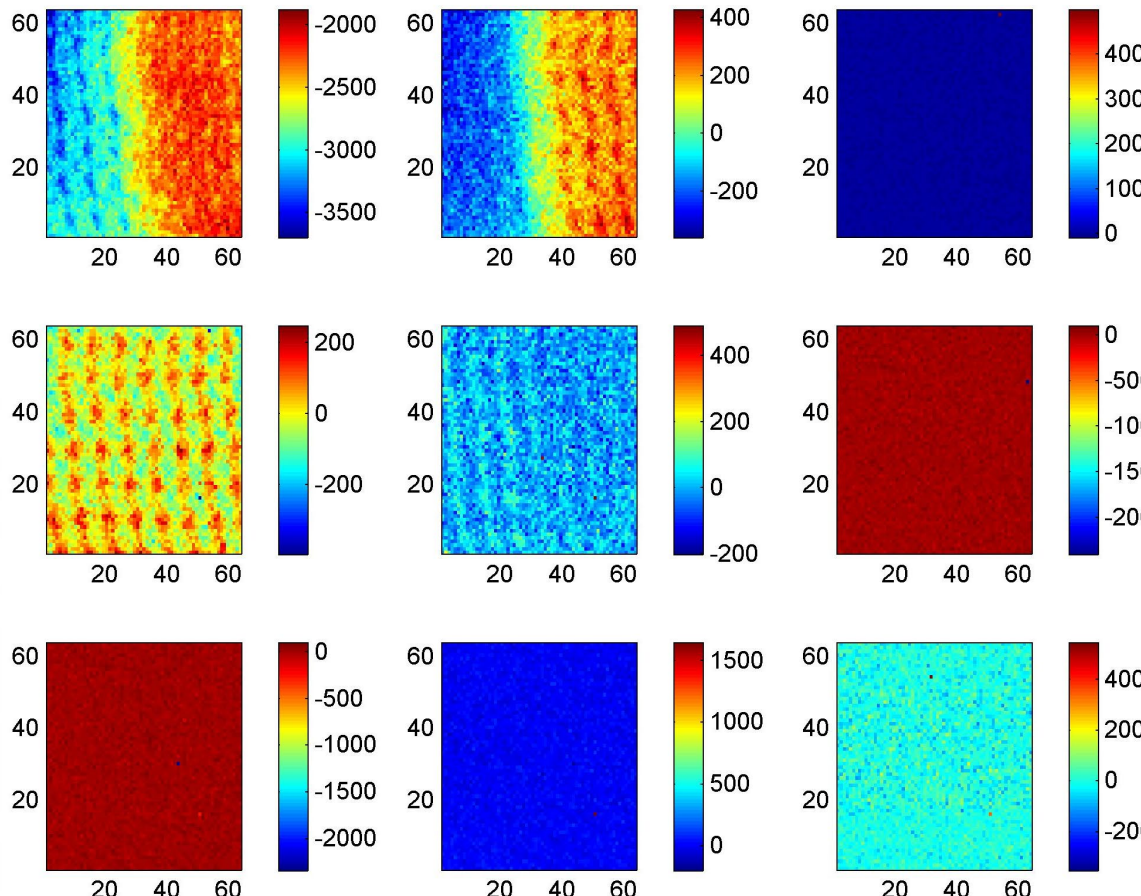


- Material:**
- STO
  - LSMO
  - BFO

If we have EELS data set, we can define three types of problems:

- **Physics based analysis:** identify compositions, orbital populations, dielectric function, etc. using known model
- **Unsupervised learning:** discover intrinsic variability in the EELS data set
- **Supervised learning:** identify EELS spectra following some examples

# EELS on the $\text{CaTiO}_3$ - $\text{SrTiO}_3$ heterostructure

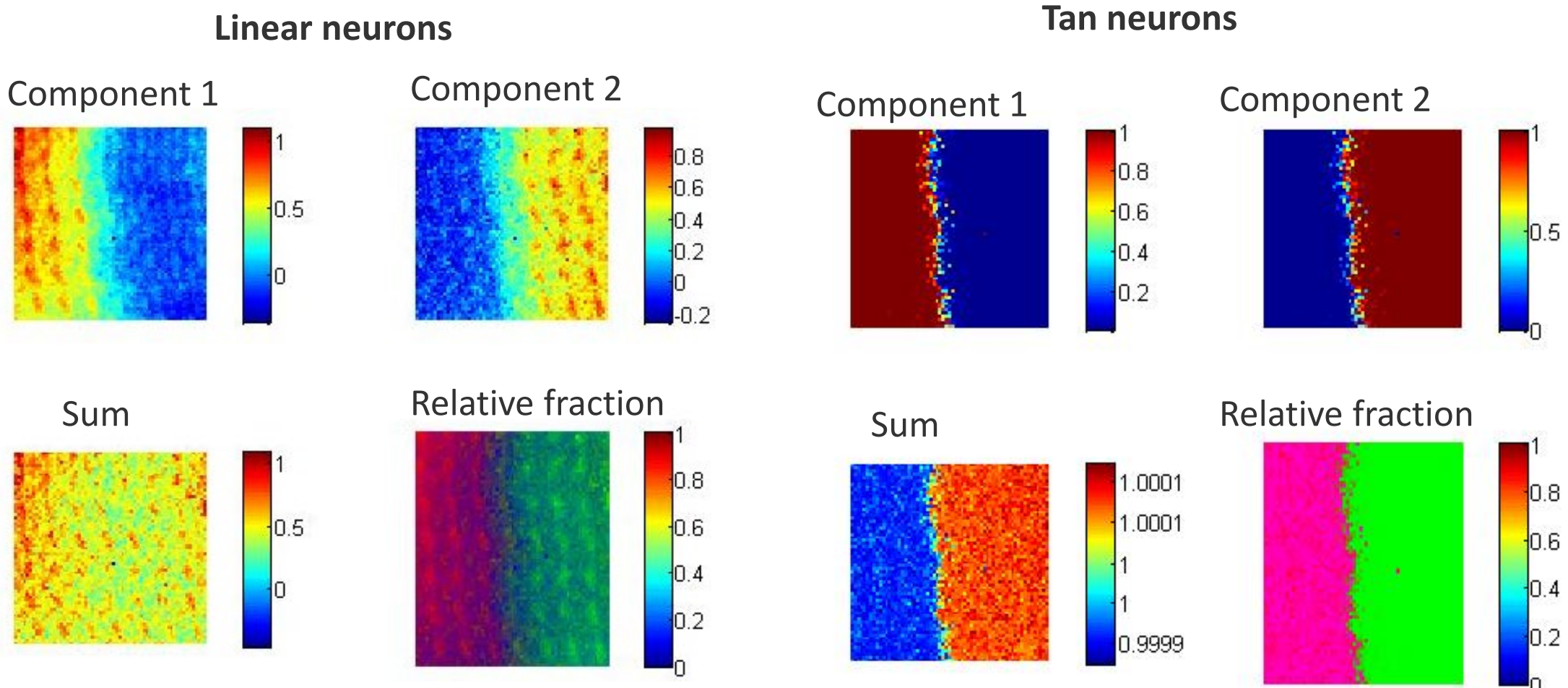


Data by A. Lupini

- Maps clearly identify components
- The subsequent maps are noise
- Note that maps without structure are dominated by outliers
- Maps show remarkable difference in contrast and symmetry

# Shallow NN Analysis

- **Training set:** subset of the image with known composition (or curated label set)
- **Recognition:** full image

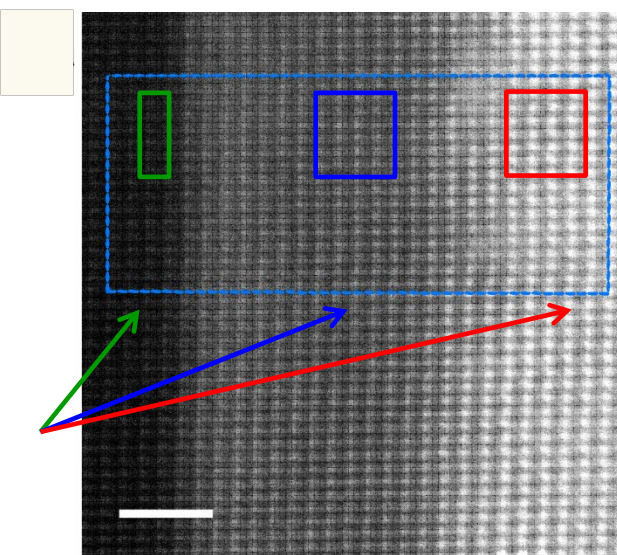


Data A. Lupini, analysis S.V. Kalinin, unpublished (2010)

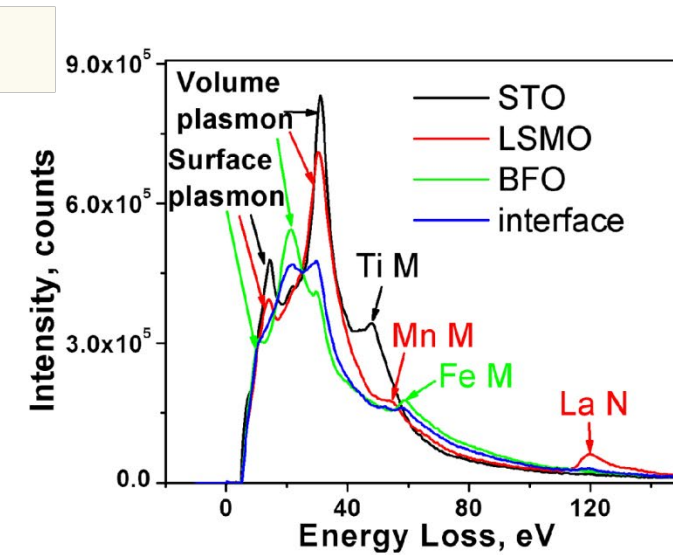
# EELS on LSMO-STO-BFO

Linear mixing  $S(x, R) = \sum_i a_i(x) w_i(R) + N$  but  $w_i(R)$  are known

STEM of STO/LSMO/BFO interface



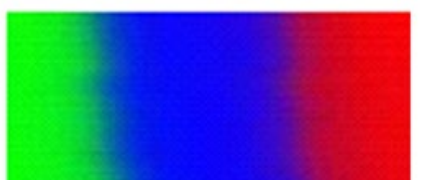
Low-loss EELS spectra of three components



Fit coefficient map

“Chemistry”

35 to 125 eV



Residuals map

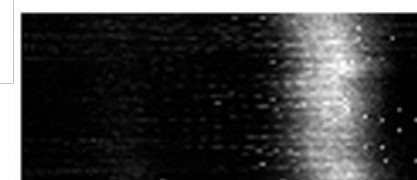
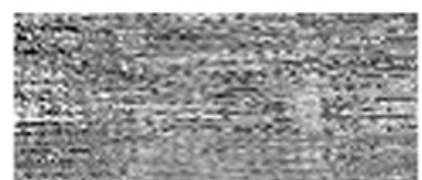
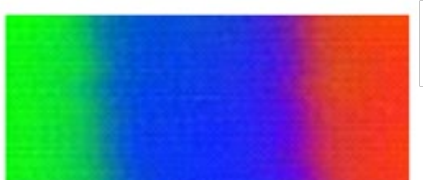


$\chi^2$  map



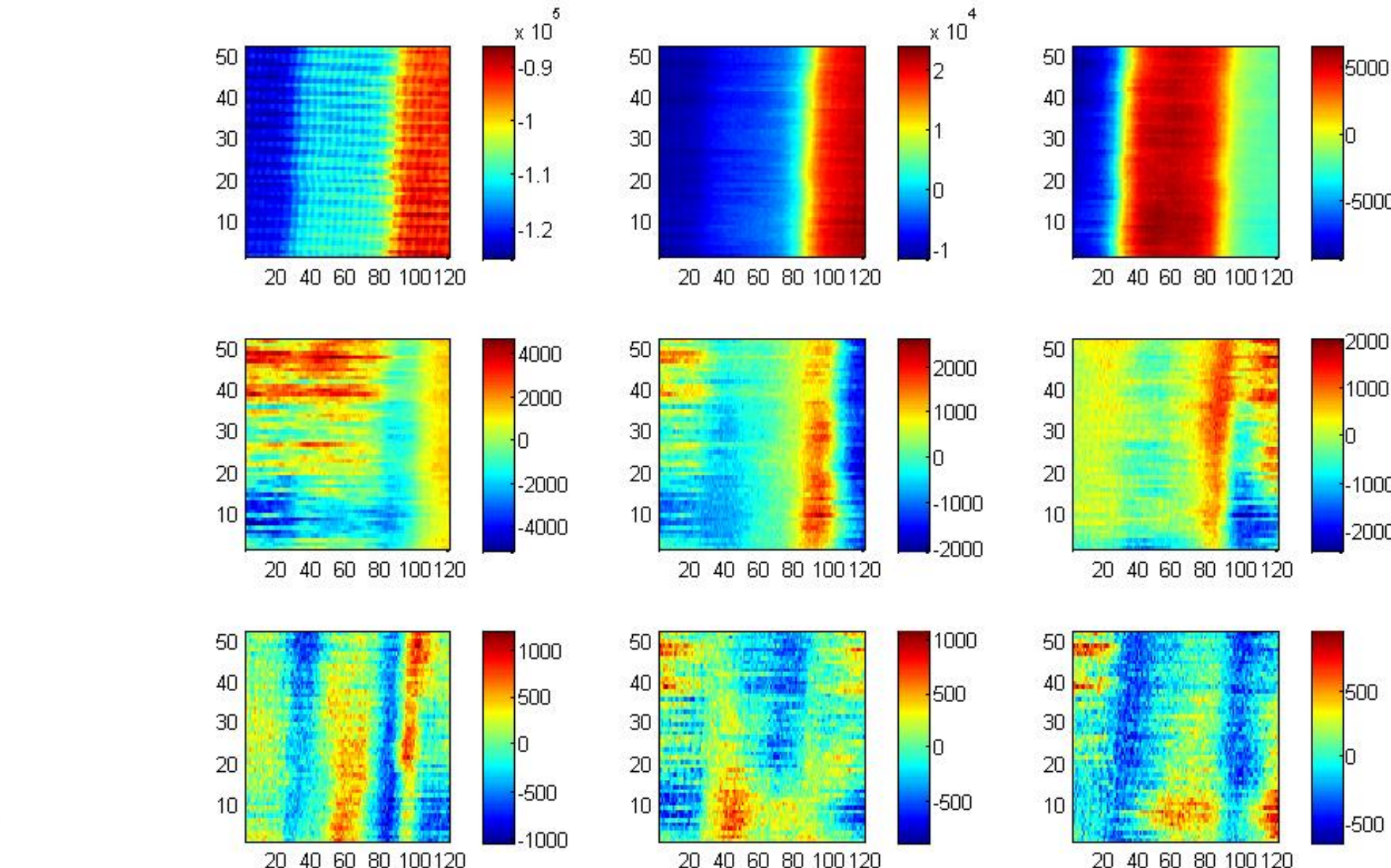
“Plasmons”

5 to 35 eV



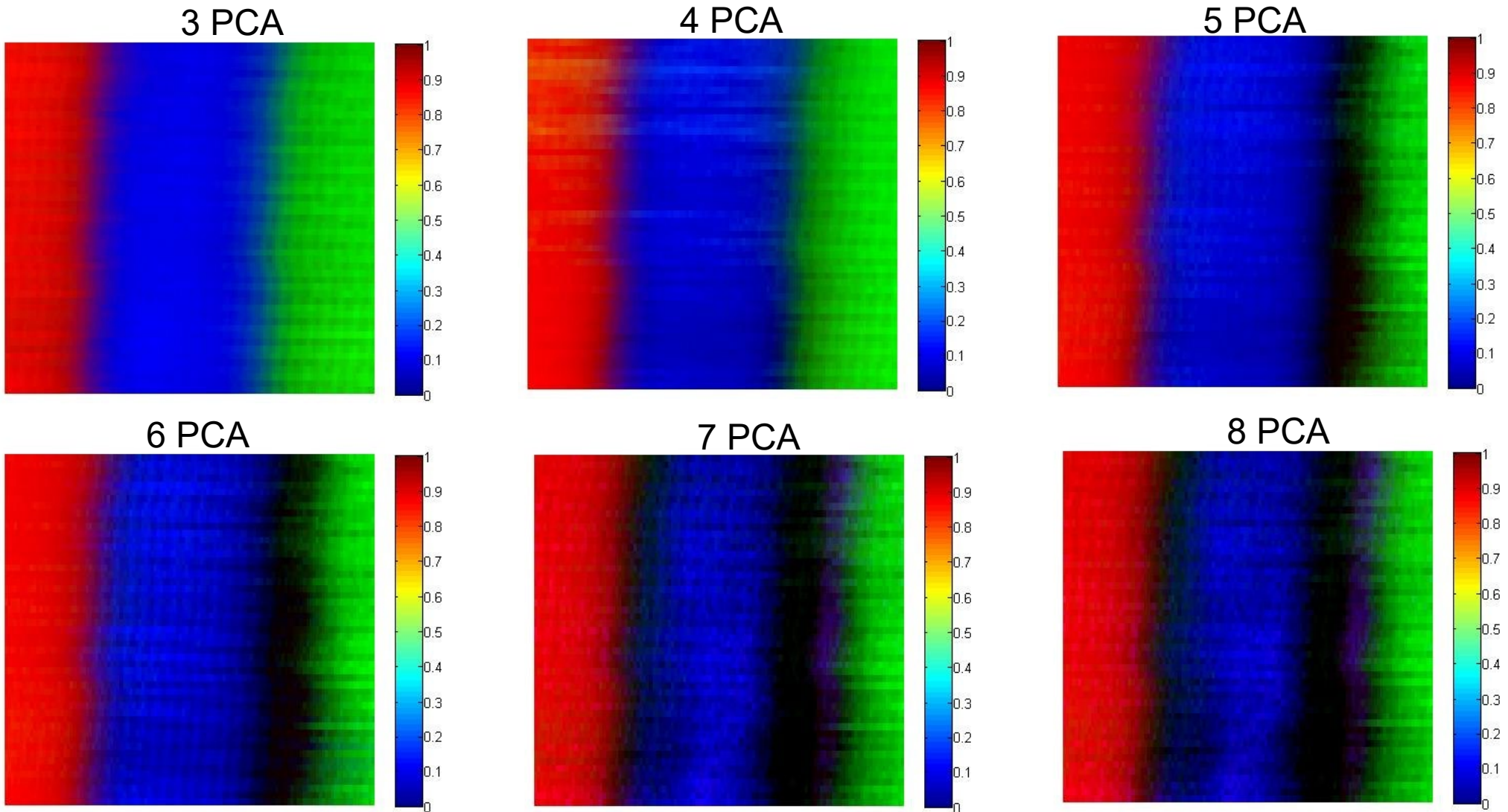
A.Y. BORISEVICH ET AL,  
Phys. Rev. Lett. **105**,  
087204 (2010).

# PCA Analysis: loadings



DATA FROM A.Y. BORISEVICH ET AL, Phys. Rev. Lett. **105**, 087204 (2010).

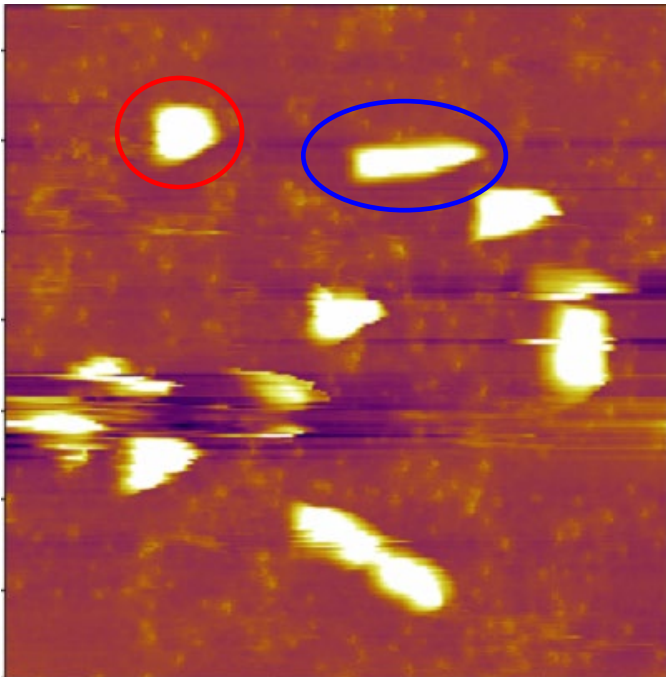
# Recognition imaging: STO – LSMO - BFO



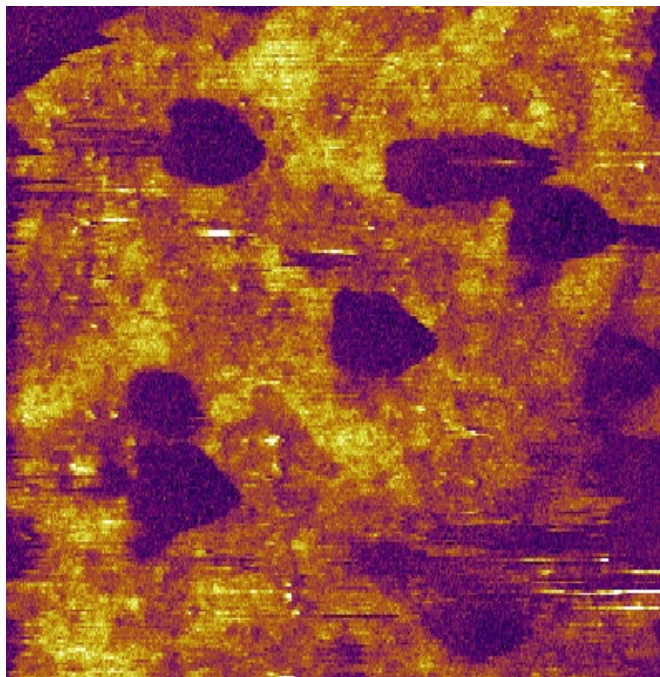
Data A. Borisevich, analysis S.V. Kalinin, unpublished (2010)

# Electromechanical probing of bacteria

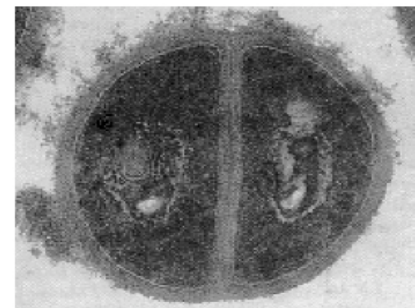
Topography



PFM Amplitude



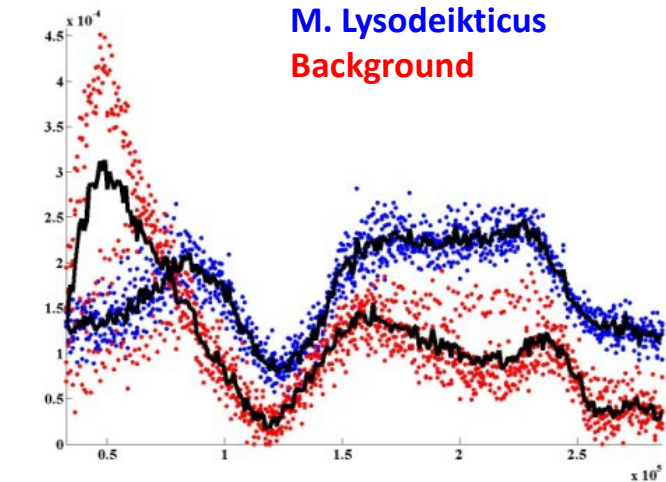
M.Lysodeikticus



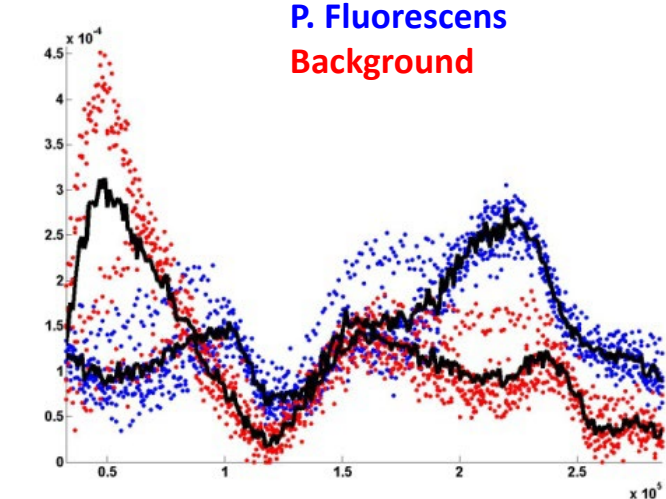
P.Fluorescens



M.P. NIKIFOROV, ET AL  
Nanotechnology **20**,  
405708 (2009).



*M. Lysodeikticus*  
Background



*P. Fluorescens*  
Background

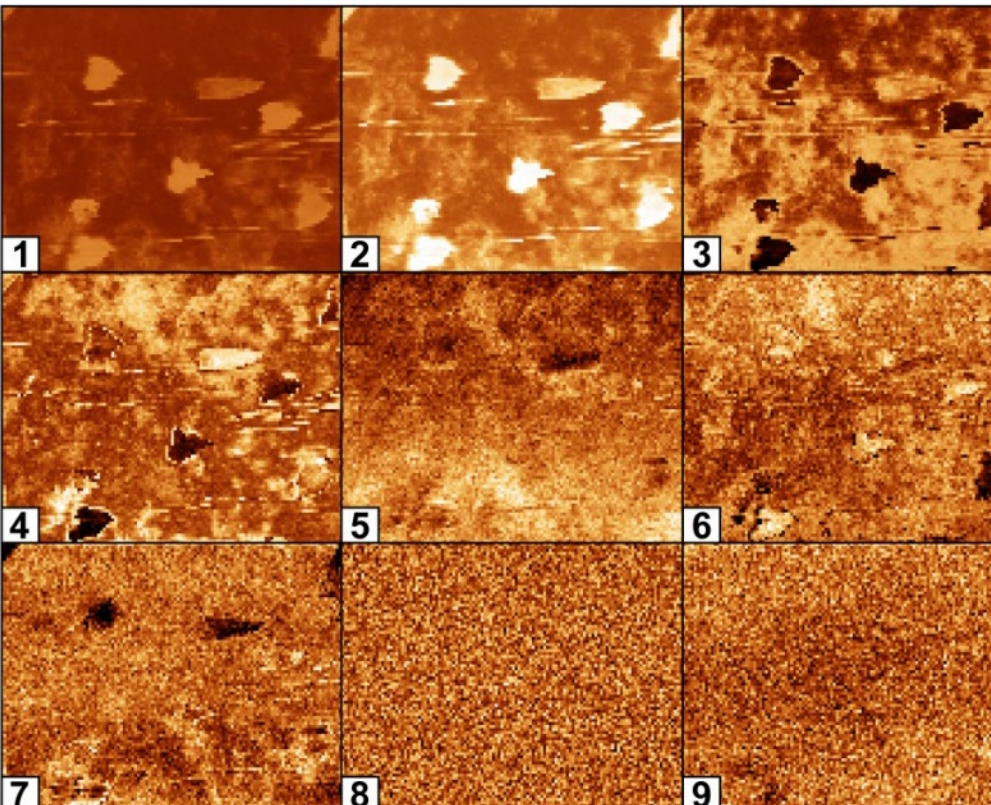
*Micrococcus Lysodeikticus*: Gram positive, spherical, aerobic bacterium

*Pseudomonas Fluorescens*: Gram-negative, rod-shaped, aerobic bacterium

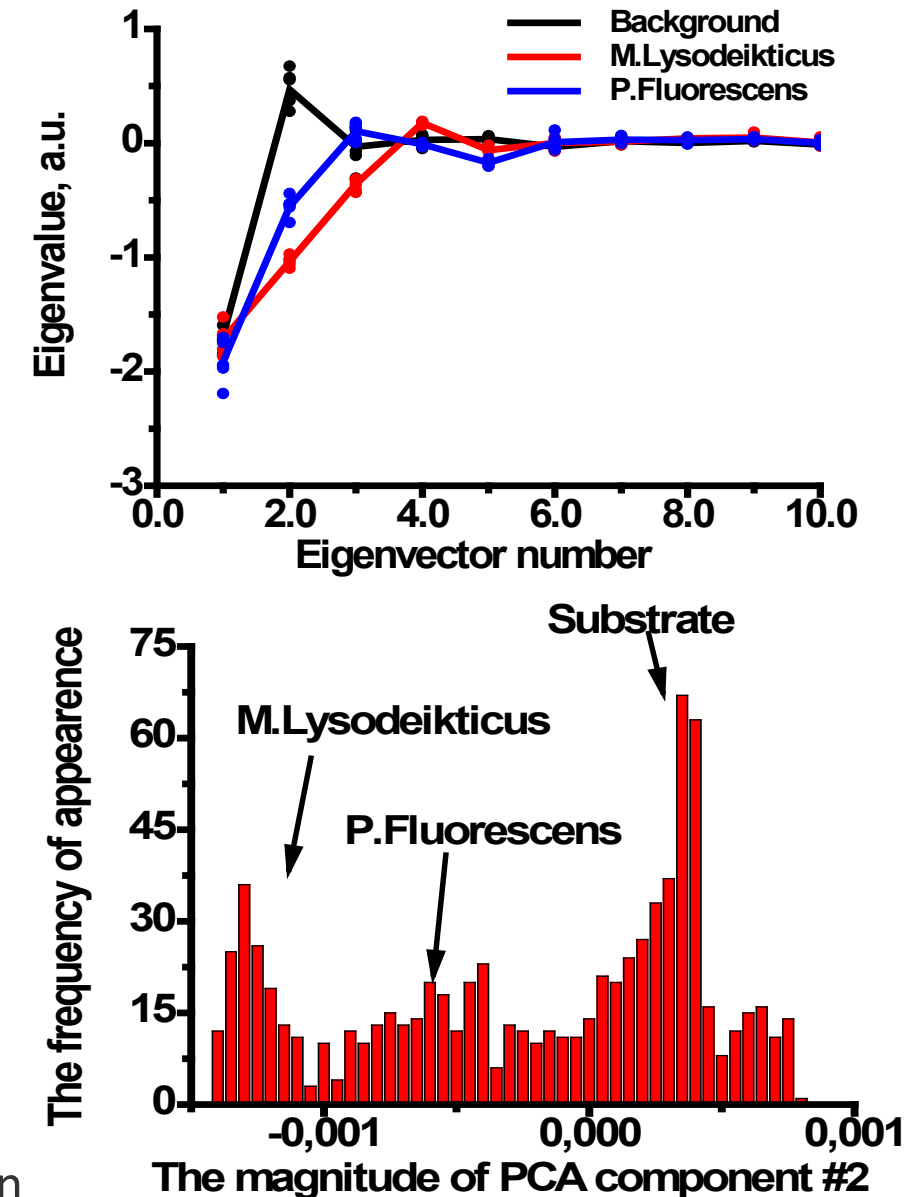
# PCA separation?

Principal component analysis:  $A_i(\omega_j) = a_{ik} w_k(\omega_j)$

$w_k(\omega)$  are found from  $\mathbf{C} = \mathbf{A}\mathbf{A}^T$

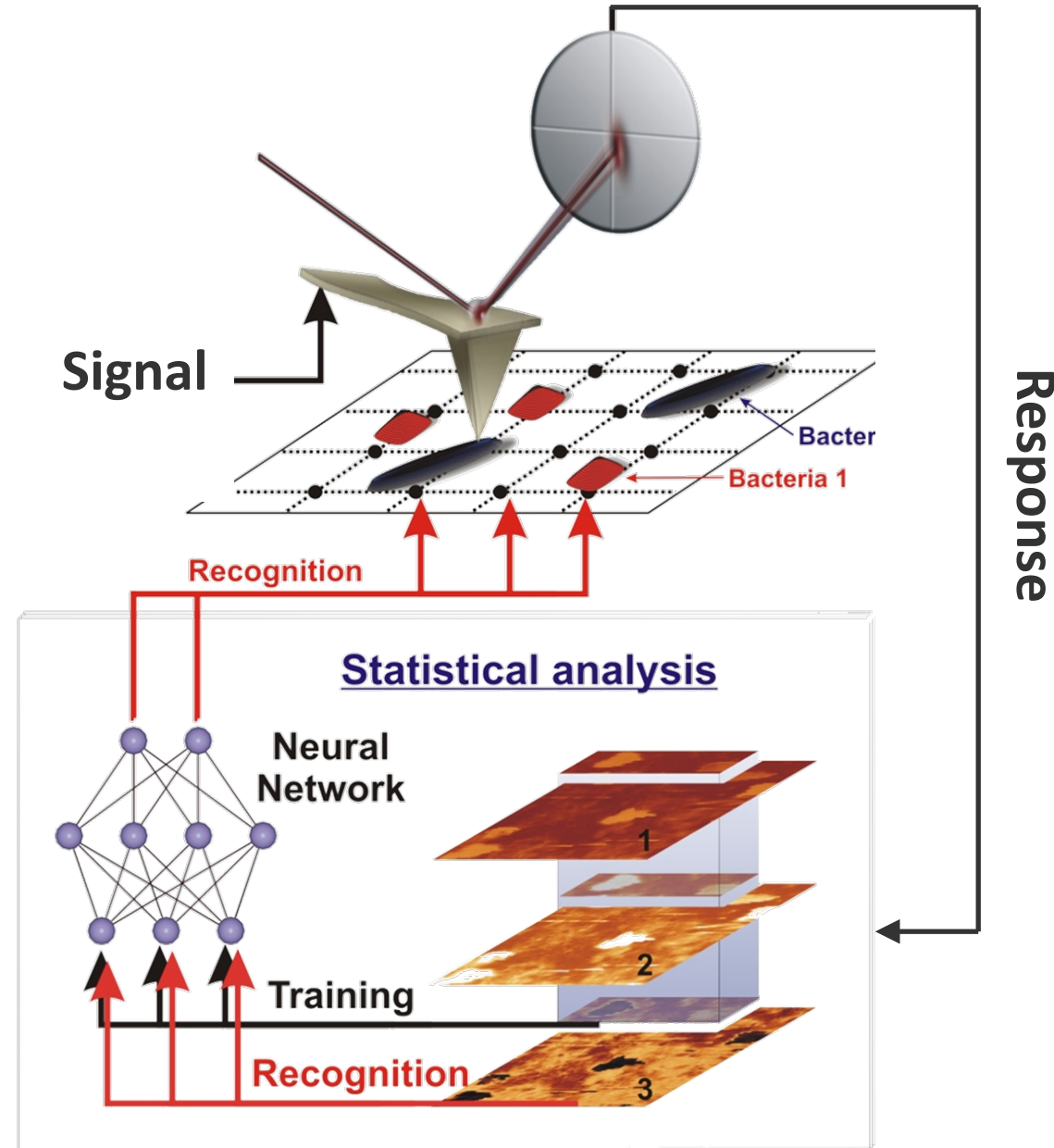


- Bacteria are differentiated on PCA maps
- One component is insufficient for unambiguous separation
- Need either shape information...
- Or all components!



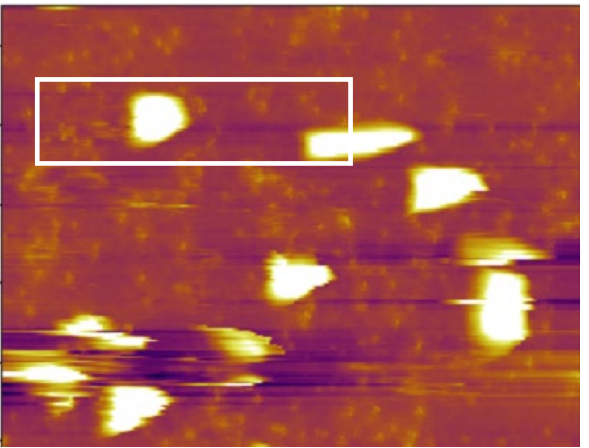
# Supervised bacteria identification

- Recognition imaging is implemented using BE PFM as signal
- However, any signal can be used: optical, mass-spectrometry, etc.
- Or any microscopic technique
- As long as labeled training set is available

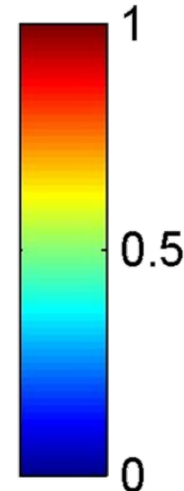
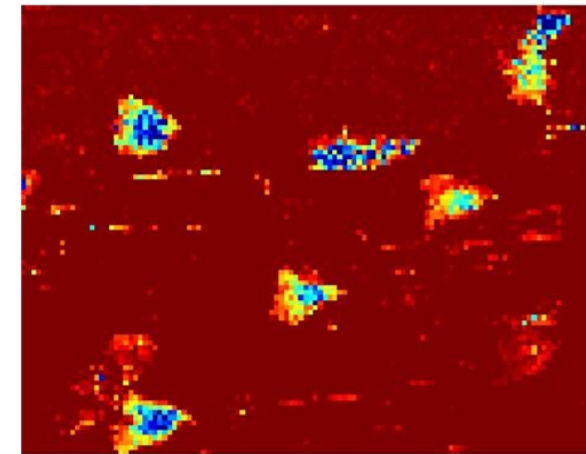


# Recognition imaging of bacteria

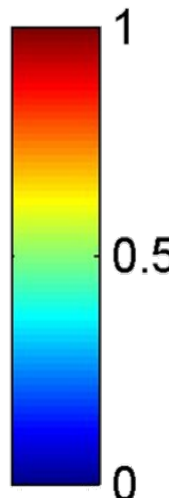
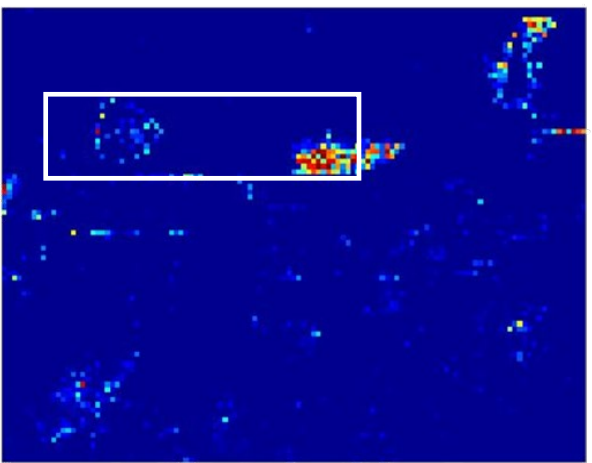
Topography



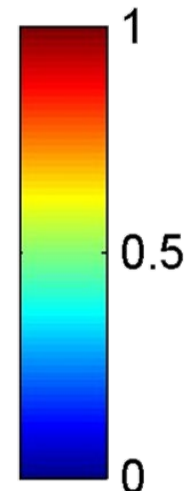
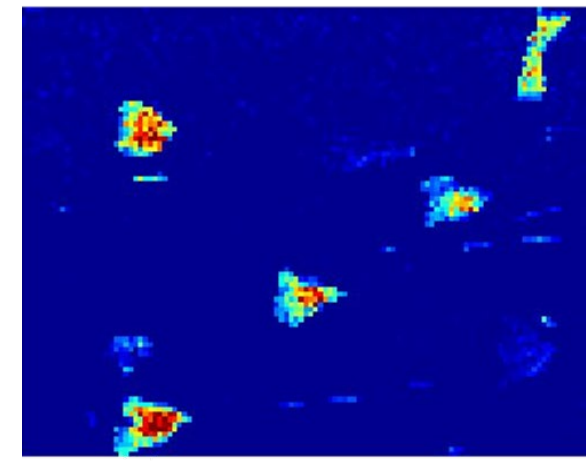
Background recognition



P. Fluorescens recognition

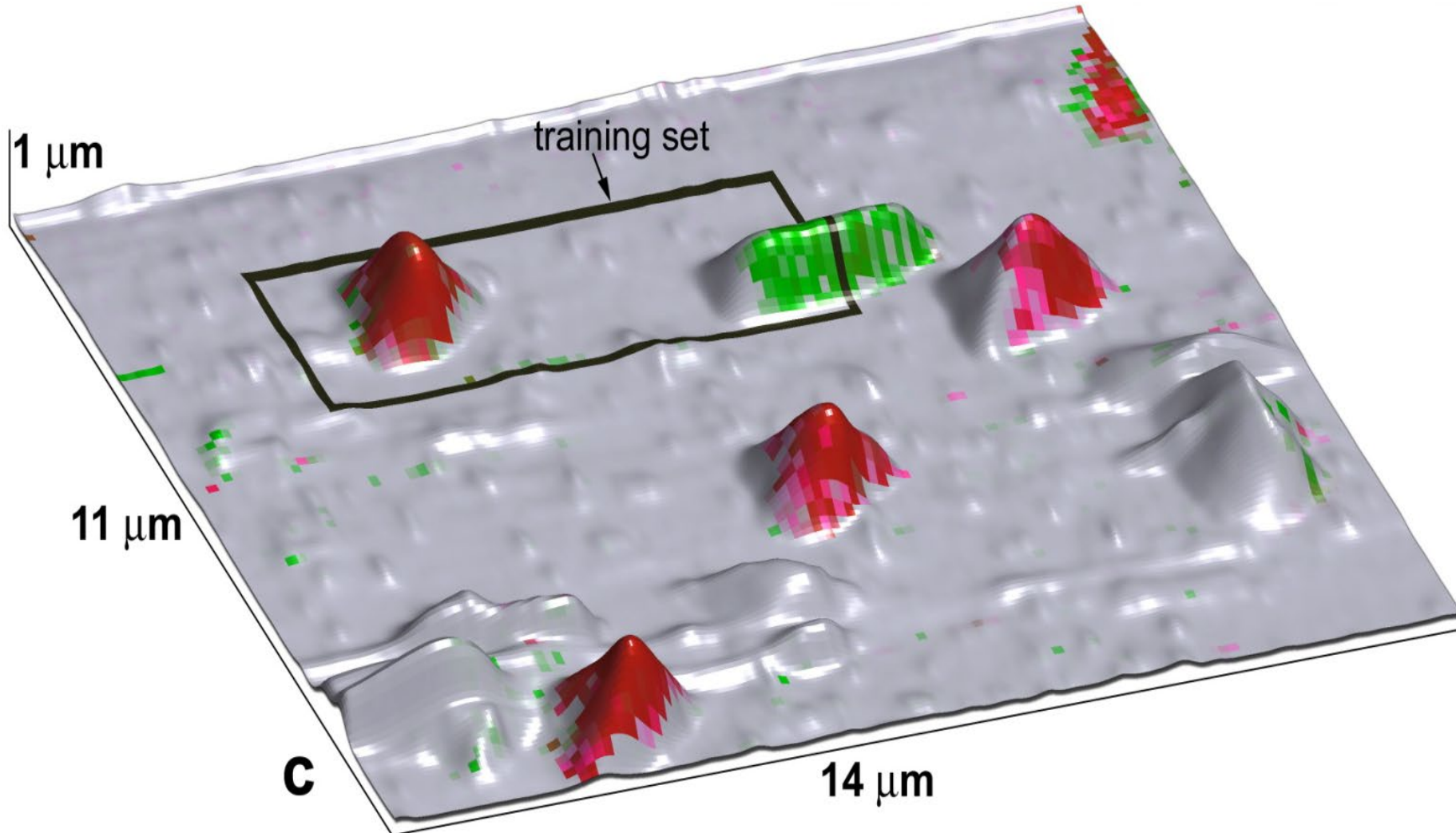


M. Lisodejicticus recognition



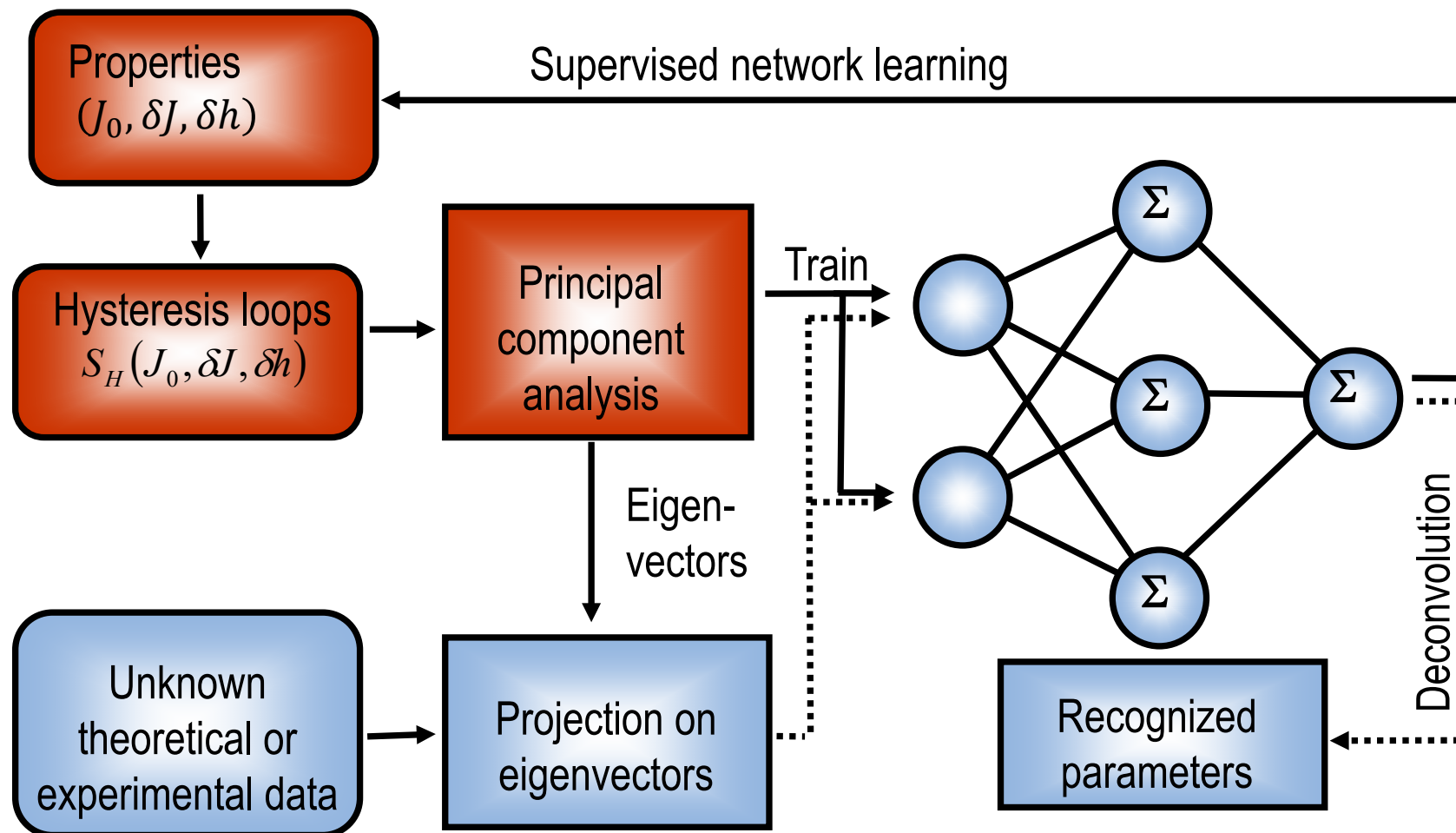
M.P. NIKIFOROV, A.A. VERTEGEL, V.V. REUKOV, G.L. THOMPSON, S.V. KALININ, and S. JESSE, *Functional recognition imaging using artificial neural networks: Applications to rapid cellular identification by broadband electromechanical response*, Nanotechnology **20**, 405708 (2009).

# Recognition imaging of bacteria



M.P. NIKIFOROV, A.A. VERTEGEL, V.V. REUKOV, G.L. THOMPSON, S.V. KALININ, and S. JESSE, *Functional recognition imaging using artificial neural networks: Applications to rapid cellular identification by broadband electromechanical response*, Nanotechnology **20**, 405708 (2009).

# Can we train NN using model?



- A ‘family’ of Ising model-based hysteresis loops of varying parameters is calculated
- An artificial neural network is then trained to recognize each theoretical loop
- The trained neural network is then applied to experimental data to extract parameters

# Ising model

**Random bond – random field Ising model**

**Glauber dynamics**

$$H(H) = \sum_{i,j} J_{ij} S_i S_j + \sum_i (h_i + H) S_i$$

$$h_{loc}^i = \sum_j J_{ij} S_j - (H + h_i) \quad h_{loc}^i S_i < 0$$

Figure by  
S. Jesse

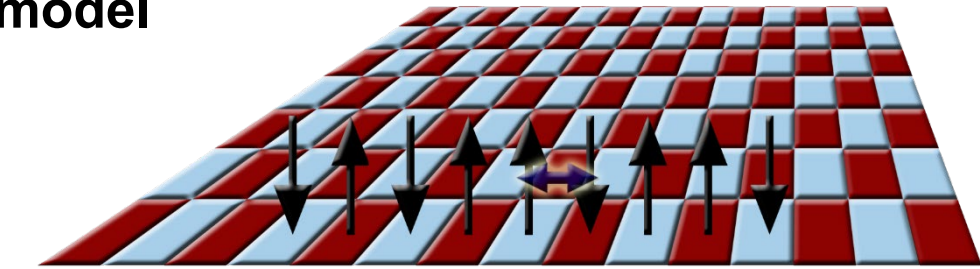
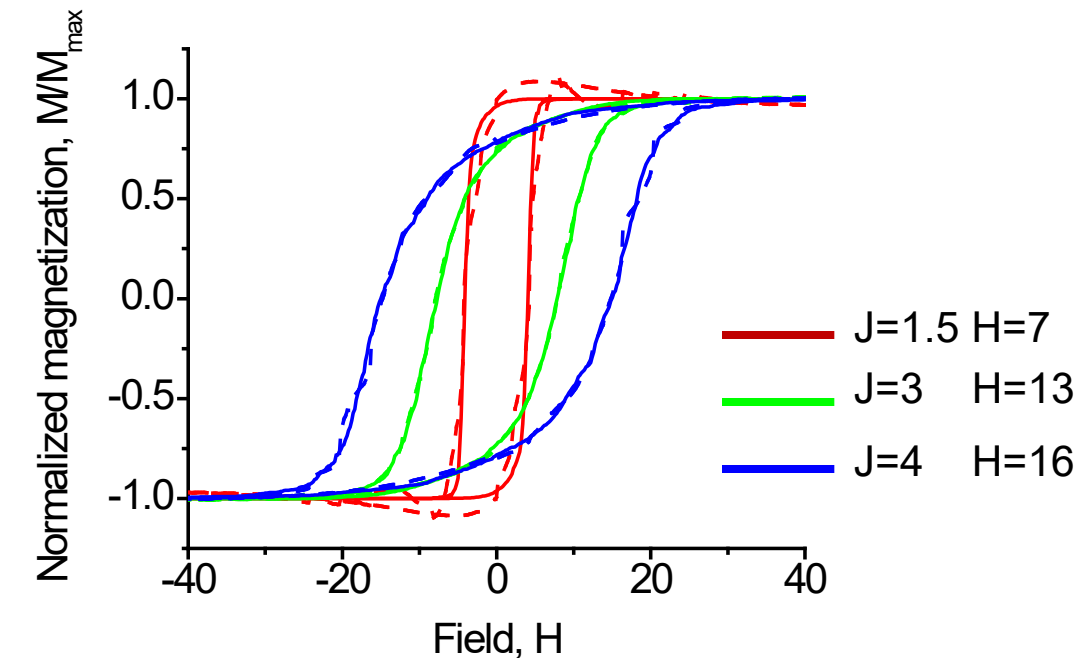
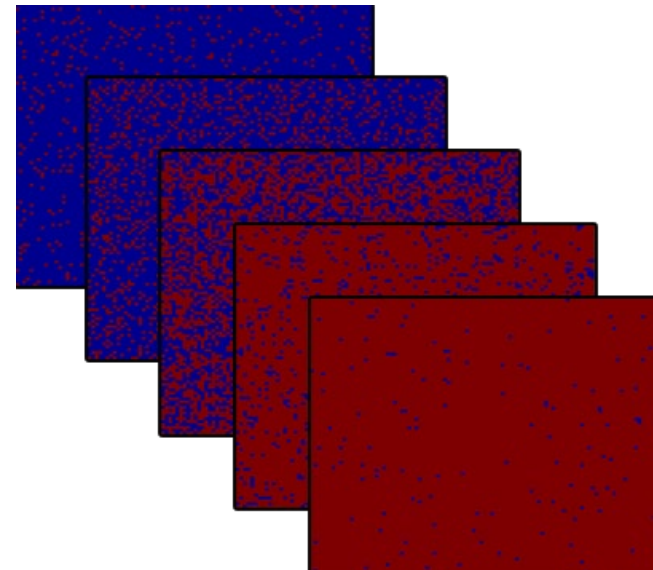
**Relate hysteresis loops generated using the Ising model**

Exchange integral –  $J_0$ ,

Random bond disorder -  $\delta J$ ,

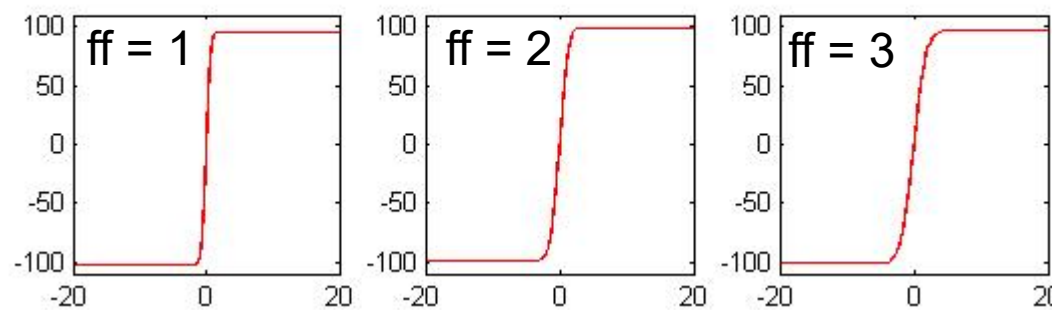
Random field disorder -  $\delta h$

**to actual experimental ferroelectric switching loops**

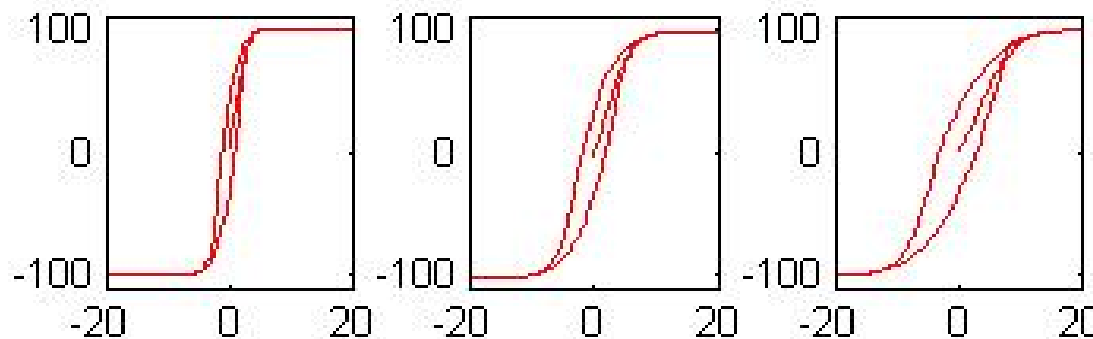


# Examples:

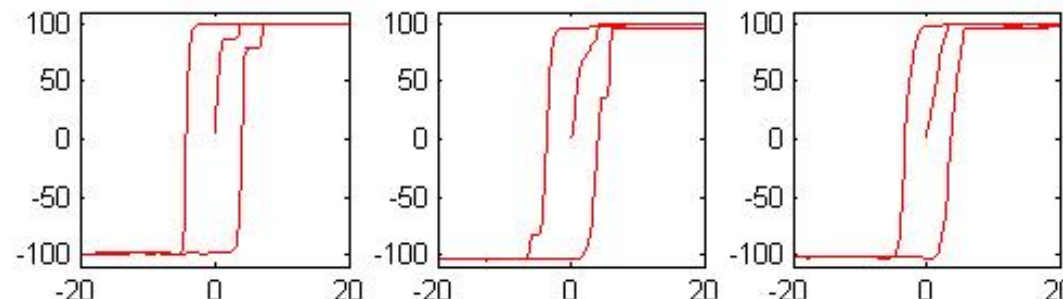
$J_0 = 0; \delta J = 0; \delta h = .5 * ff;$



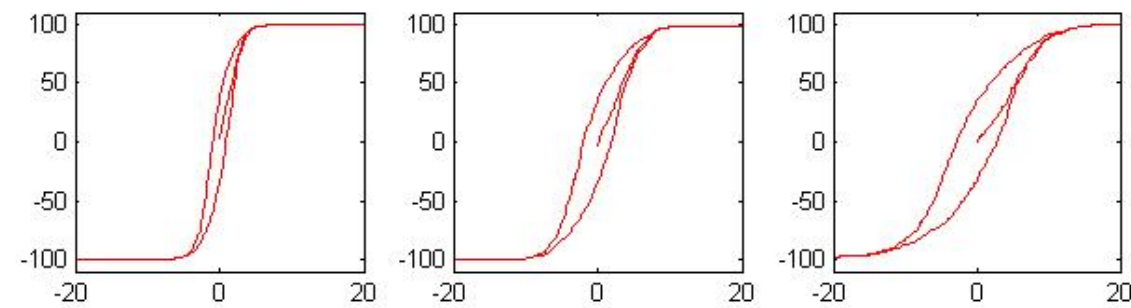
$J_0 = 0; \delta J = .5 * ff; \delta h = 0;$



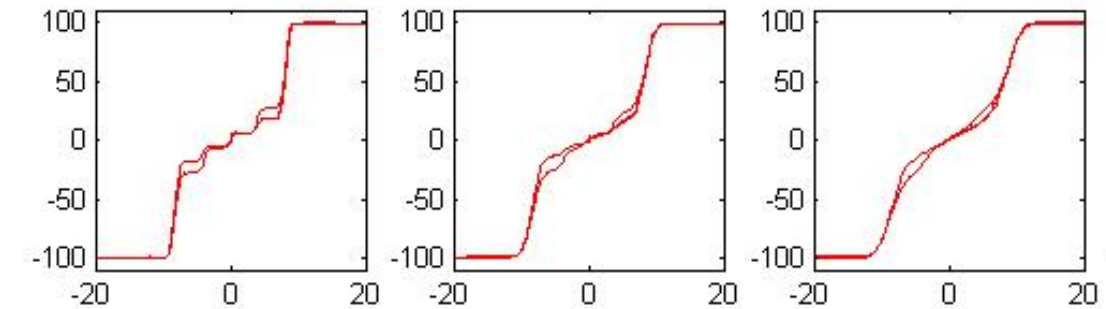
$J_0 = 1; \delta J = 0; \delta h = .5 * ff;$



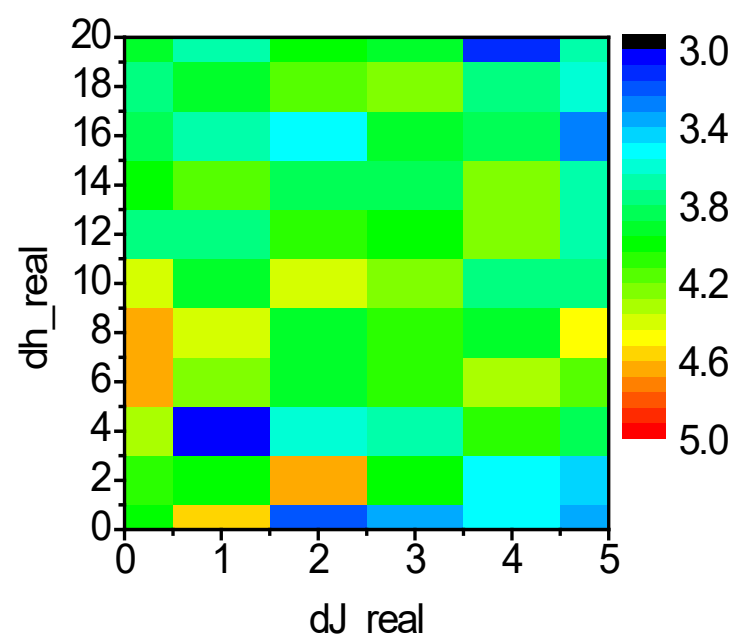
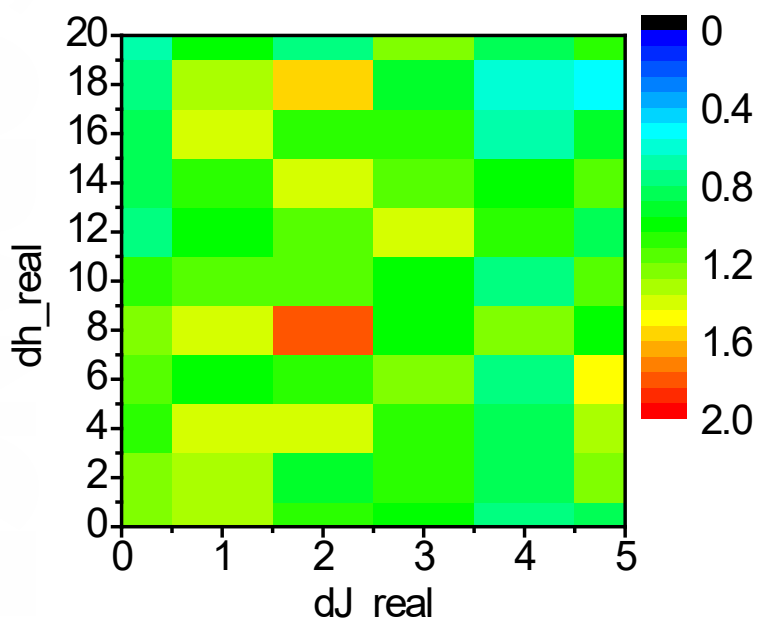
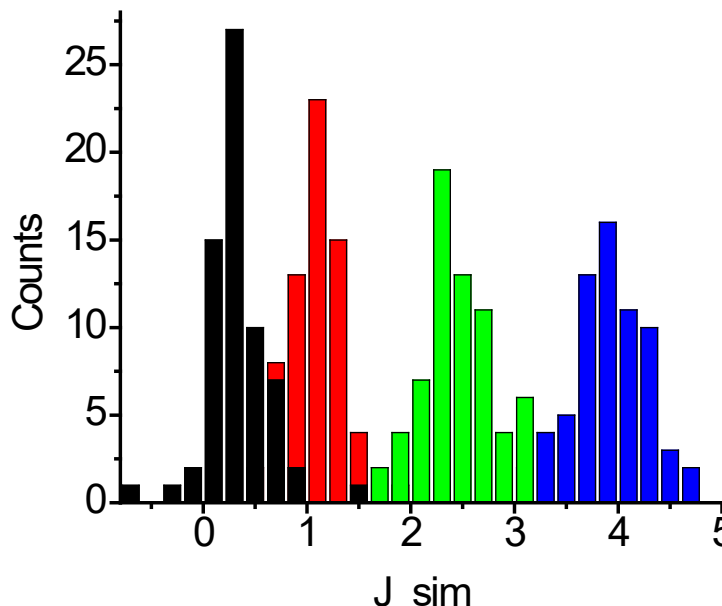
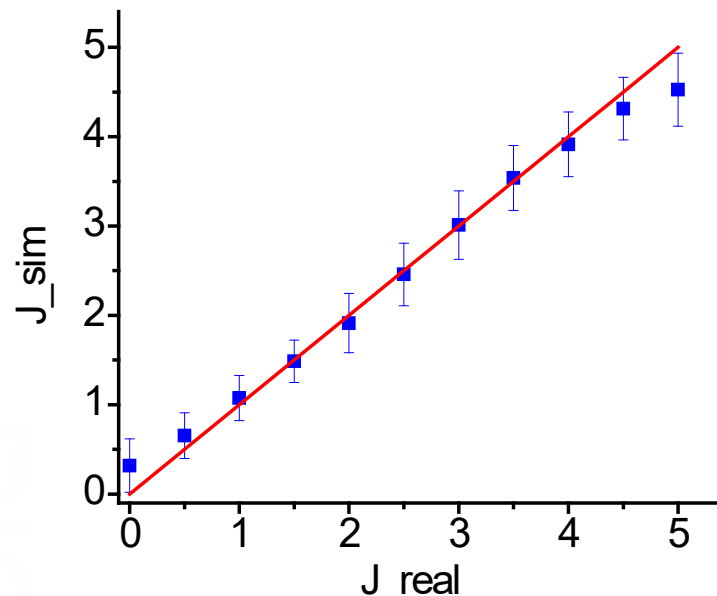
$J_0 = 0; \delta J = .5 * ff; \delta h = .5 * ff;$



$J_0 = -1; \delta J = 0; \delta h = .5 * ff;$

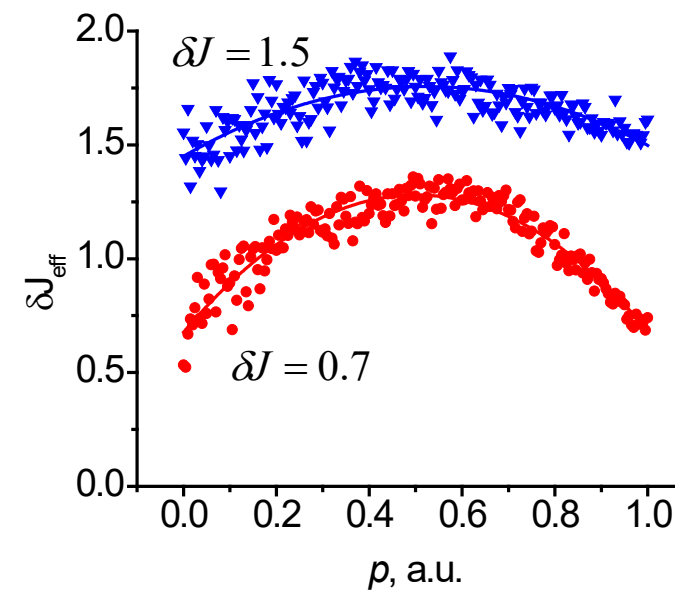
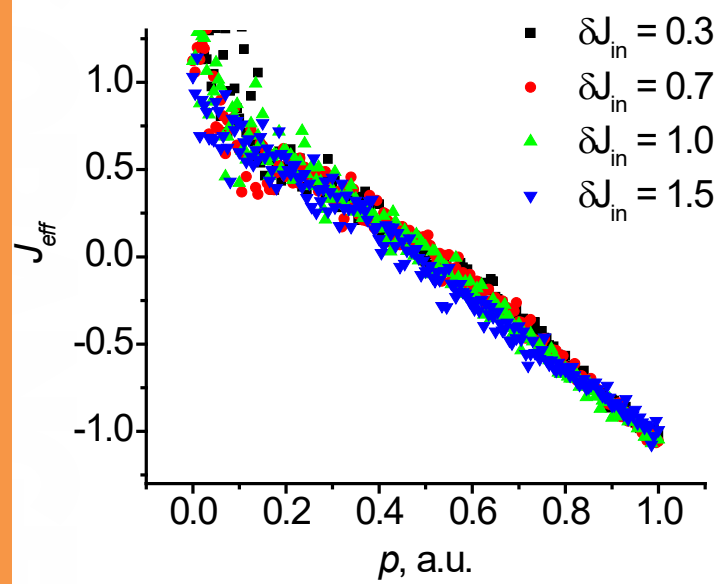
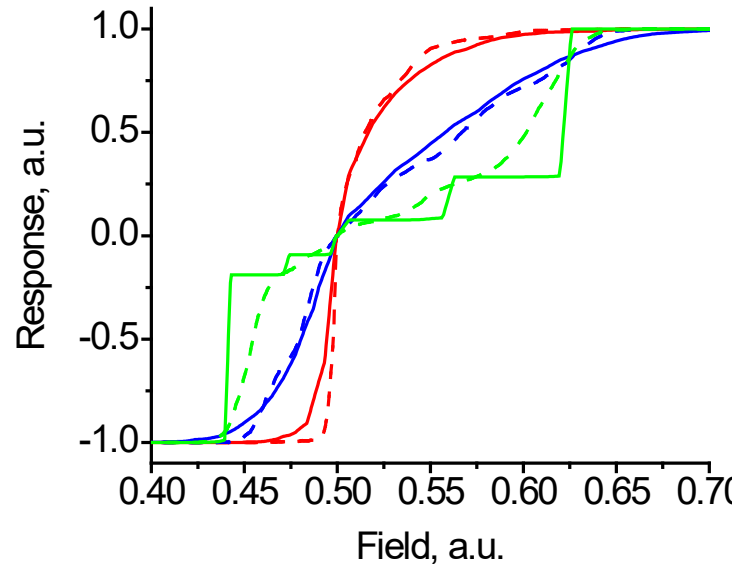
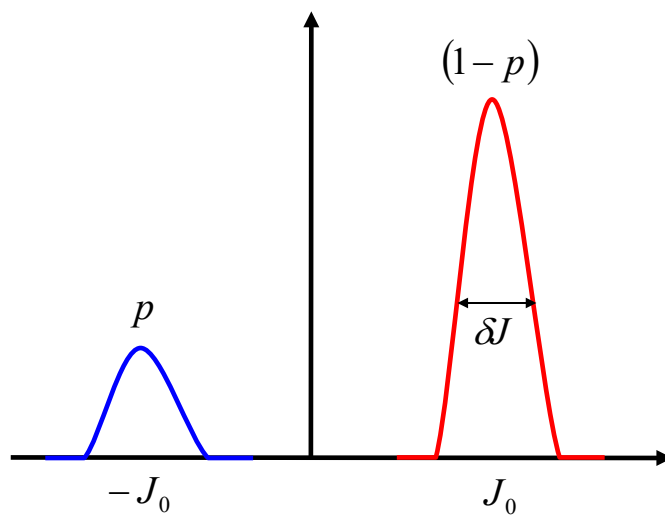


# Self-recognition of Ising model



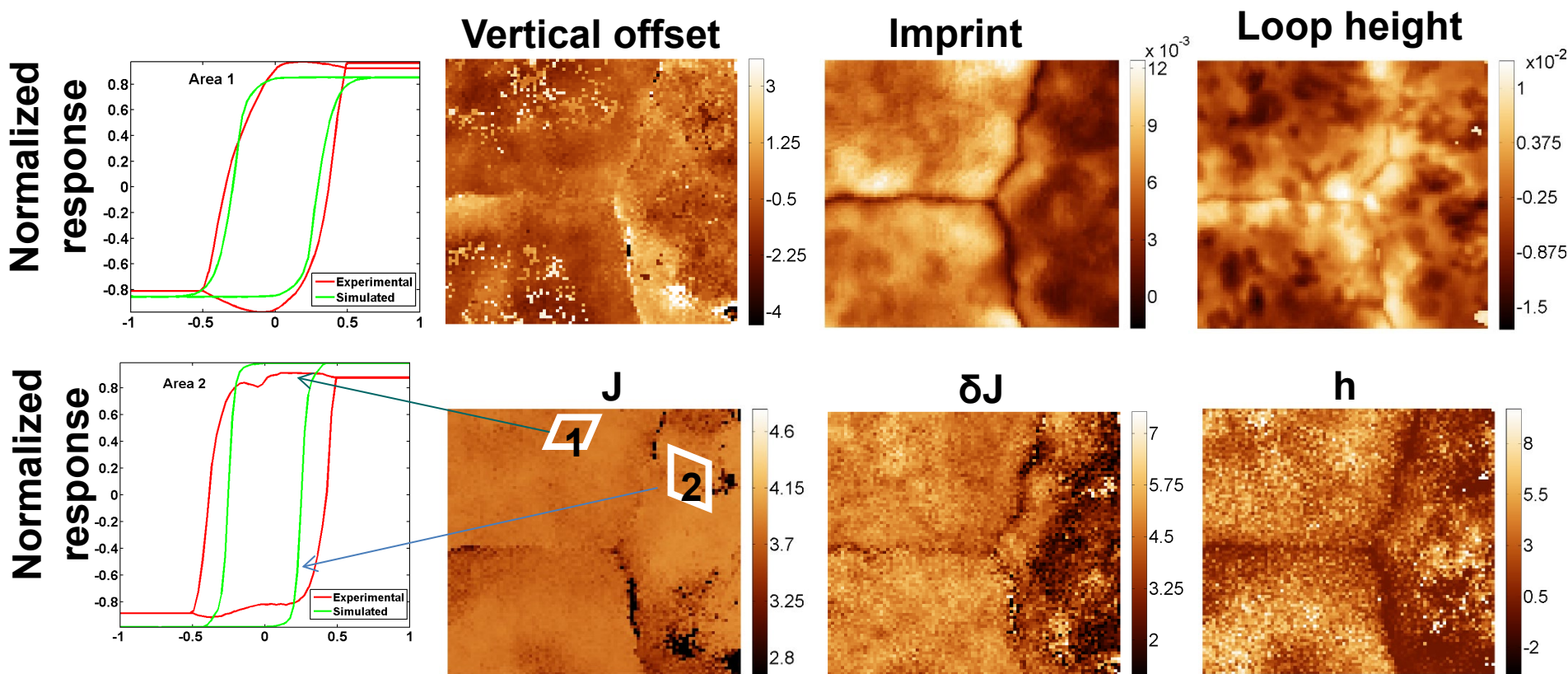
O.S. OVCHINNIKOV, S. JESSE, P. BINTACCHIT,  
S. TROLIERMCKINSTRY, and S.V. KALININ,  
*Disorder identification in hysteresis  
data: recognition analysis of random-  
bond random-field Ising model*, Phys.  
Rev. Lett. **103**, 157203 (2009).

# Recognition of more complex model



O.S. OVCHINNIKOV, S. JESSE, P. BINTACCHIT, S. TROLIER MCKINSTRY, and S.V. KALININ, *Disorder identification in hysteresis data: recognition analysis of random-bond random-field Ising model*, Phys. Rev. Lett. **103**, 157203 (2009).

# Analysis of loops based on Ising model



- A ‘family’ of Ising model based hysteresis loops of varying parameters is calculated
- An artificial neural network is then trained to recognize each theoretical loop
- The trained neural network is then applied to experimental data to extract parameters

A. KUMAR, O. OVCHINNIKOV, S. GUO, F. GRIGGIO, S. JESSE, S. TROLIER-MCKINSTRY, and S.V. KALININ, *Spatially Resolved Mapping of Disorder Type and Distribution in Random Systems using Artificial Neural Network Recognition*, Phys. Rev. B **84**, 024203 (2011).